Chapter 3 : Results and Discussion

(A) Surface Tension Measurements

Surface Tension

The surface properties of the aqueous binary surfactant mixtures : $Cu(C_{12}tmed)(acac)Cl$ with SDS , CTAB and $C_{12}E_8$ were studied by surface tension measurements . The measurements were carried out as a function of the mole fraction of $[Cu(C_{12}tmed)(acac)Cl]$ in 0.1 M NaCl solution under atmospheric pressure and at a constant temperature T .

Surface tension studies of individual surfactant in water

Graph of surface tension versus ln [surfactant] for different surfactants in water were shown in Figure 3-01.

(i) Critical Micelle Concentration , CMC

The CMC was obtained from the point of intersection of two linear portions of the curve . From the γ-ln C plot , the straight line portion of the curve ($\gamma < 60$ $mN\,m^{-1}$) was fitted to the data by the method of least squares with the equation :

$$\gamma = K_i \ln C + const \qquad (3\text{-}01)$$

where K_i is the slope of γ-ln C plot .

(ii) Surface excess concentration , Γ

For a dilute solution of ionic surfactant , the surface excess concentration is given by Gibbs adsorption equation.

$$\Gamma = -\frac{1}{aRT}\left(\frac{d\gamma}{d\ln C}\right) \qquad (3\text{-}02)$$

where $a = 2$ for 1 : 1 ionic compound .

$a = 3$ for 1 : 2 ionic compound .

The value $a = 2$ was used in the calculation as $Cu(C_{12}tmed)(acac)Cl$, SDS and CTAB are 1 : 1 (A^+B^-) electrolytes .

For dilute solutions of nonionic surfactant , or for a 1:1 ionic surfactant in the presence of a swamping electrolyte containing a common non-surfactant ion , the surface excess is given by equation 3-03 [1(d)] .

$$\Gamma = -\frac{1}{RT}\left(\frac{d\gamma}{d\ln C}\right) \qquad (3\text{-}03)$$

(iii) Area per molecule at the interface , A

The surface area per molecule at the interface (in nm^2) is calculated from the surface excess concentration .

$$A = \frac{10^{18}}{N\Gamma} \qquad (3\text{-}04)$$

where

N = Avogadro's number

Γ = surface excess (in $mol\,m^{-2}$) .

This can provide information on the degree of packing of the adsorbed surfactant molecule .

(iv) Surface pressure at CMC , π^{CMC}

Surface pressure at the critical micelle concentration is given by

$$\pi^{CMC} = \gamma_0 - \gamma^{CMC} \qquad (3\text{-}05)$$

where

γ_0 = surface tension of water

γ^{CMC} = surface tension at the CMC

The calculated results and literature values are summarized in Tables 3-01 and 3-02 .

The CMC value of each surfactant in water obtained agrees quite well with reported value , except for $C_{12}E_8$ where the purity of chemical is ≥ 98% , and was used without further purification . CMC's of Cu(C_{12}tmed)(acac)Cl and CTAB are lower than SDS , indicating that they are more surface active than SDS . The surface areas per molecule of SDS , CTAB and $C_{12}E_8$ are around 0.55-0.65 nm^2 , while Cu(C_{12}tmed)(acac)Cl (1.07 nm^2) is the largest among the surfactants studied . The larger surface area of Cu(C_{12}tmed)(acac)Cl is due to the bulky head group , which consists of ligands ethylenediamine and acetylacetonate .

(v) Surface tension studies of individual surfactant in 0.1M NaCl

Experimental values obtained for surfactants studied in the presence of 0.1 M NaCl are shown in Table 3-03 .

The presence of electrolyte reduces the CMC of both ionic and nonionic surfactants . For the ionic surfactant , the depression of the CMC is due mainly to the decrease in the thickness of the ionic atmosphere surrounding the ionic head groups in the presence of the additional electrolyte and the consequent decreased electrostatic

repulsion between them in the micelle . For nonionic surfactant , the electrolyte has the effect of "salting in" and "salting out" of the hydrophobic groups . The decrease of CMC is due to salting out of the monomeric form of surfactant and thus favoring the micellization [1(d)].

Surface area also decreases in the presence of electrolytes , which may be the result of compression of the electrical double layer surrounding the charged head groups .

Addition of electrolyte results in increased adsorption at the aqueous solution-air interface because of the decrease of the repulsion between the oriented ionic heads at the interface when the ionic strength of the solution is increased [1(d)].

Surface tension studies of binary surfactant in 0.1M NaCl

The surface tension values of the mixed surfactant solutions with various mole fractions of $Cu(C_{12}tmed)(acac)Cl$ are plotted against the total concentrations of surfactants in Figures 3-02 to 3-04 : Figure 3-02 $Cu(C_{12}tmed)(acac)Cl$ - SDS system ; Figure 3-03 $Cu(C_{12}tmed)(acac)Cl$ - CTAB system and Figure 3-04 $Cu(C_{12}tmed)(acac)Cl$ - $C_{12}E_8$ system . In all cases , surface tension value decreases with increasing concentration , but remains constant above the critical micelle concentration (CMC) . In Cu / SDS mixtures , the surface activity of each binary mixtures under investigation is much greater than the surface activity of individual components . The ability to decrease the surface tension is stronger as the binary system approaches equimolar mixing .

Surface pressure and surface tension at CMC (π_{12}^{CMC} and γ_{12}^{CMC})

Figure 3-05 shows the π_{12}^{CMC} and γ_{12}^{CMC} values for different mixed surfactant system . It is noteworthy that in the case of $Cu(C_{12}tmed)(acac)Cl$ - SDS system , the surface tension values of the mixture at the CMC , γ_{12}^{CMC} , is always lower than the pure surfactant alone , i.e. γ_1^{CMC} and γ_2^{CMC} . The maximum deviation from ideality can be seen when mixing ratio approaches 1:1 . In the case of $Cu(C_{12}tmed)(acac)Cl$ - CTAB system , γ_{12}^{CMC} decreases monotonously with increasing mole fraction of $Cu(C_{12}tmed)(acac)Cl$. For $Cu(C_{12}tmed)(acac)Cl$ - $C_{12}E_8$ system , γ_{12}^{CMC} is almost constant at the value of pure $C_{12}E_8$ when the mole fraction of $Cu(C_{12}tmed)(acac)Cl$ increases from 0 to until approximately 0.8 , after which it increases to that of the pure Cu(II) micelle .

Total surface excess and average surface Area (Γ_t and A_{av})

For the mixed surfactant system of SDS and $Cu(C_{12}tmed)(acac)Cl$ at a constant ionic strength (0.1 M NaCl) and a mixing ratio ,

$$Cu(C_{12}tmed)(acac)Cl \rightleftharpoons Cu(C_{12}tmed)(acac)^+ + Cl$$
$$NaDS \rightleftharpoons Na^+ + DS^- \qquad (3\text{-}06)$$

The total surface excess is given by Gibbs adsorption equation [22(f)]

$$\Gamma_t = -\frac{1}{RT}\left(\frac{d\gamma}{d\ln C_t}\right)_\alpha \qquad (3\text{-}07)$$

where

α = mole fraction of surfactant 1 in the total surfactant concentration

Γ_t = total surface excess concentration

C_t = total surfactant concentration

The average surface area per molecule A_{av} , in nm^2 , when Γ_t , is $mol\,m^{-2}$ is given by

$$A_{av} = \frac{10^{18}}{N\Gamma_t} \qquad (3\text{-}08)$$

where

N = Avogadro's number

Graph of average surface area for mixed surfactant system is shown in Figure 3-06 .

As can be seen from Figure 3-06 , the average surface areas for the mixed surfactant system are much lower than the pure surfactant alone when the co-surfactant is SDS , but they fall in the range of pure surfactants when the co-surfactant is CTAB and $C_{12}E_8$. The average surface area for the mixed Cu-SDS is in the range of 0.18-0.24 nm^2 , compared to 0.43 nm^2 (Cu) and 0.38 nm^2 (SDS) . The decrease of surface area shows surface molecules are tightly packed , due to attractive interaction of oppositely charged head groups .

CMC of mixed surfactant solutions C_{12}^M

Graphs of C_{12}^M versus mole ratio of Cu in the total surfactant concentration for the mixed surfactant system are shown in Figures 3-07 to 3-09 . When SDS is the co-surfactant , critical micelle concentration for the mixture , C_{12}^M is very much lower when compared to either surfactant alone , i.e. C_1^M and C_2^M , but when CTAB and $C_{12}E_8$ are the co-surfactants , the C_{12}^M falls between the CMC of the individual surfactants .

Table 3-01 : Some surface properties of individual surfactants in water

Surfactant	T (°C)	CMC ($mol\,dm^{-3}$)	Γ_{max} ($10^6\ mol\,m^{-2}$)	A_{min} (nm^2)	π^{CMC} ($mN\,m^{-1}$)
$Cu(C_{12}tmed)(acac)Cl$	20	9.2×10^{-4}	1.6	1.07	30.5
SDS	25	8.0×10^{-3}	2.8	0.59	33.9
CTAB	22	9.2×10^{-4}	3.1	0.54	31.5
$C_{12}E_8$	22	8.6×10^{-4}	2.5	0.65	35.6

Table 3-02 : Literature values of surface properties of individual surfactants in water

Surfactant	T (°C)	CMC ($mol\,dm^{-3}$)	Γ_{max} ($10^6\ mol\,m^{-2}$)	A_{min} (nm^2)	π^{CMC} ($mN\,m^{-1}$)
$Cu(C_{12}tmed)(acac)Cl$	25	9.4×10^{-4} [11(d)]	1.5	1.09	32.0
SDS	25	8.2×10^{-3} [92]	3.2	0.53	32.5
CTAB	25	9.1×10^{-4} [93]	-	-	-
$C_{12}E_8$	25	1.09×10^{-4} [94]	2.5	0.66	37.2

Table 3-03 : Some surface properties of individual surfactants in 0.1M NaCl

Surfactant	T (°C)	CMC ($mol\,dm^{-3}$)	Γ_{max} ($10^6\ mol\,m^{-2}$)	A_{min} (nm^2)	π^{CMC} ($mN\,m^{-1}$)
$Cu(C_{12}tmed)(acac)Cl$	20	1.81×10^{-4}	3.9	0.43	34.2
SDS	20	1.17×10^{-3}	4.4	0.38	37.4
CTAB	22	7.29×10^{-5}	3.7	0.45	32.6
$C_{12}E_8$	22	9.17×10^{-5}	3.0	0.56	36.2

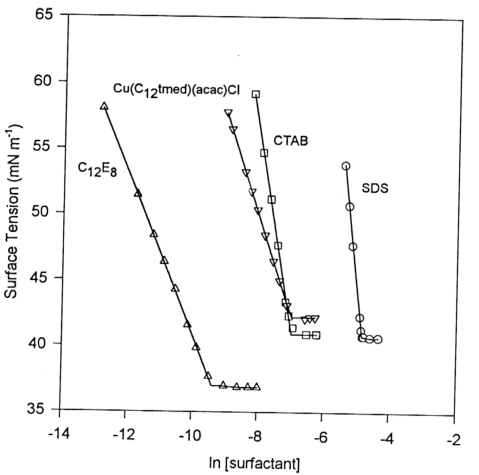

Figure 3-01 : Plot of surface tension against ln [surfactant] in water

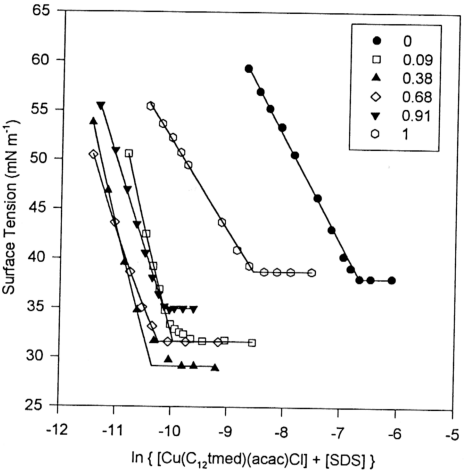

Figure 3-02 : Plot of surface tension against the total surfactant concentration for $Cu(C_{12}tmed)(acac)Cl$ and SDS in 0.1M NaCl at 20°C , where the overall mole fraction of $Cu(C_{12}tmed)(acac)Cl$ is kept constant on each curve .

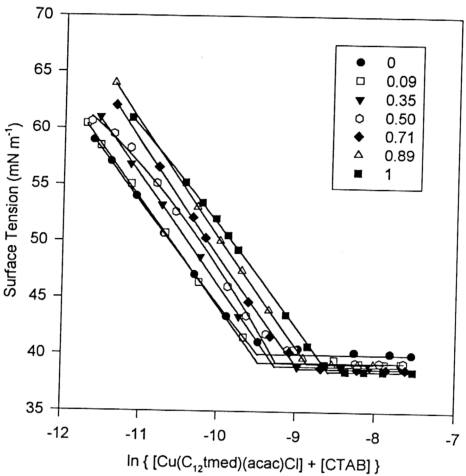

Figure 3-03 : Plot of surface tension against the total surfactant concentration for $Cu(C_{12}tmed)(acac)Cl$ and CTAB in 0.1M NaCl at 22°C , where the overall mole fraction of $Cu(C_{12}tmed)(acac)Cl$ is kept constant on each curve .

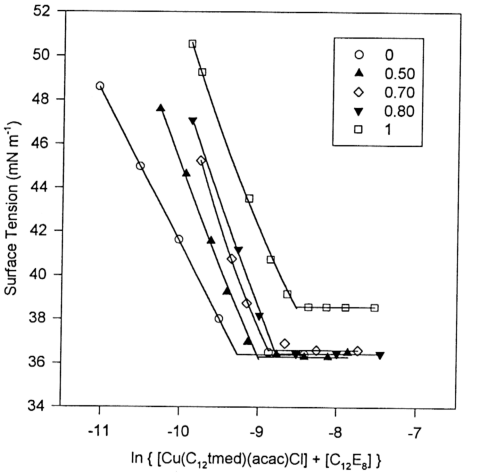

Figure 3-04 : Plot of surface tension against the total surfactant concentration for $Cu(C_{12}tmed)(acac)Cl$ and $C_{12}E_8$ in 0.1M NaCl at 23°C , where the overall mole fraction of $Cu(C_{12}tmed)(acac)Cl$ is kept constant on each curve .

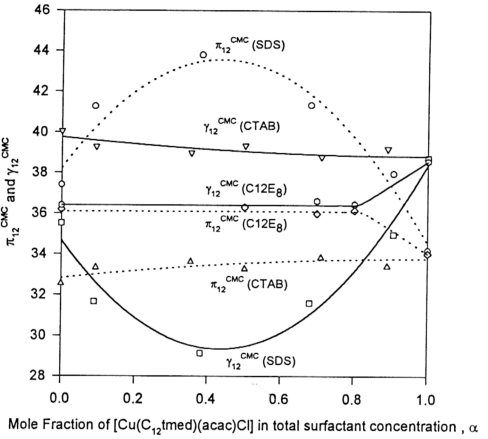

Figure 3-05 : π_{12}^{CMC} (.....) and γ_{12}^{CMC} (___) of different mixed surfactant systems .

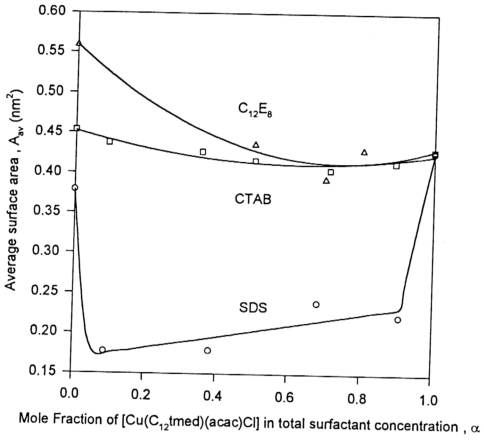

Figure 3-06 : Average surface areas for different mixed surfactant systems

(I) Regular Solution Approach

The composition and mutual interaction of the components in mixed micelle [21] and mixed monolayer [22(f)] formation can be calculated by using the Regular Solution model .

Micellar interaction parameter , β^M

Nonideality due to interactions between different surfactant components in the mixed micelles is measured by the micellar interaction parameter β^M .

$$\beta^M = \frac{\ln\left[\frac{\alpha C_{12}^M}{x^M C_1^M}\right]}{\left(1-x^M\right)^2} = \frac{\ln\left[\frac{(1-\alpha)C_{12}^M}{(1-x^M)C_2^M}\right]}{\left(x^M\right)^2} \qquad (3\text{-}09)$$

where

C_1^M , C_2^M , C_{12}^M = CMC of pure surfactants 1 , 2 and their mixture

α = mole fraction of surfactant 1 in the total mixed surfactants

x^M = mole fraction of surfactant 1 in the mixed micelles

β^M = interaction parameter for the mixed micelles

Micellar mole fraction x^M and interaction parameter β^M for Cu / SDS , Cu / CTAB and Cu / $C_{12}E_8$ systems are shown in Tables 3-04(a) to 3-04(c) . Figures 3-06 to 3-08 show plots of CMC of mixtures C_{12}^M as a function of monomer composition α for various surfactant mixtures . The predicted CMC mixtures values shown by the line are

calculated by fitting average β^M values into equation 3-09 . Figure 3-10 shows plots of micellar composition x^M as a function of monomer composition α for various surfactant mixtures .

β^M value

Both Cu / CTAB and Cu / $C_{12}E_8$ systems gives average β^M values close to zero , *viz.* , -0.12 and -0.13 respectively . However, for Cu / CTAB system , there is a gradual decrease of β^M value from 0.17 to -0.35 as α increases .The interaction of the two different surfactants with each other in mixed micelles is not very different from their interactions with themselves before mixing . Mixed cationic-anionic micelles (Cu / SDS system) exhibit large negative deviation from ideality , with β^M = -10.9 . This implies a fairly strong interaction between the ionic head groups of Cu and SDS in the mixed micelles . Strong interaction occurs due to the attraction of oppositely charged head groups between cationic and anionic surfactant molecules .

Data show that molecular interaction between two surfactants in mixed micelle formation decreases in the order : Cu / SDS >> Cu / $C_{12}E_8$ ≈ Cu / CTAB .

In Cu / SDS mixtures , from the x^M values , we can see that the mixed micelles formed in the wide composition range (α) , contain nearly equal quantities of surface active anions and cations . This is possible due to formation of electroneutral combinations of ions . In binary system $R^+ Cl^-$ / $R^- Na^+$ (where R^+ and R^- are the surfactant molecules respectively) , there are four combination ions : $R^+ Cl^-$, $R^- Na^+$, Na^+Cl^- and R^+R^- . Na^+Cl^-

is non surface active (not forming micelle) , therefore the other new electroneutral combination R^+R^- must consequently be far more surface active than either $R^+ Cl^-$, $R^- Na^+$ and cause the decrease in CMC values . Formation of micelle from mixed solution will tend to produce a 1 : 1 ratio of the long-chain ions with negligible amounts of $R^+ Cl^-$ and $R^- Na^+$ even when the bulk mixing ratio is far from equimolar . Therefore for all mixed solutions , with bulk mixing ratios varying from 0.1 to 0.9 , the micellar composition of anionic and cationic is close to 1 : 1 .

In Cu / CTAB and Cu / $C_{12}E_8$ mixtures , the x^M values increase monotonically with increasing mole fraction of Cu in the total mixing concentration . The mixed micelles behave thermodynamically like ideal mixtures .

Table 3-04(a) : Micellar mole fraction and interaction parameter for mixed surfactant system $Cu(C_{12}tmed)(acac)Cl$ and SDS

α	β^M	x^M
0.09	-11.5	0.48
0.38	-10.8	0.55
0.68	-10.3	0.60
0.91	-10.8	0.66
Average	$-10.9 \pm 0.3^*$	-

* Average deviation is used to indicate uncertainty

Note : β^M for $\alpha = 0.5$ was not possible to obtain because of turbidity formation

Table 3-04(b) : Micellar mole fraction and interaction parameter for mixed surfactant system $Cu(C_{12}tmed)(acac)Cl$ and CTAB

α	β^M	x^M
0.09	0.1_7	0.03
0.35	0.1_8	0.16
0.50	-0.1_9	0.30
0.71	-0.2_0	0.50
0.89	-0.5_5	0.72
Average	$-0.1_2 \pm 0.2_3$	-

Table 3-04(c) : Micellar mole fraction and interaction parameter for mixed surfactant system $Cu(C_{12}tmed)(acac)Cl$ and $C_{12}E_8$

α	β^M	x^M
0.50	-0.2_2	0.35
0.70	-0.2_5	0.54
0.80	0.0_8	0.68
Average	$-0.1_3 \pm 0.1_4$	-

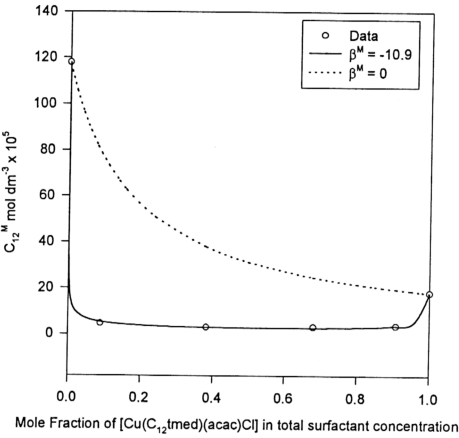

Figure 3-07 : C_{12}^{M} vs. mole fraction of [$Cu(C_{12}tmed)(acac)Cl$] in total surfactant concentration of mixed surfactant system with SDS as co-surfactant .

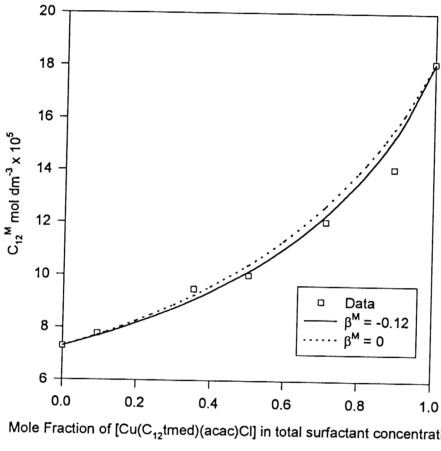

Figure 3-08 : C_{12}^{M} vs. mole fraction of [Cu(C_{12}tmed)(acac)Cl] in total surfactant concentration of mixed surfactant system with CTAB as co-surfactant .

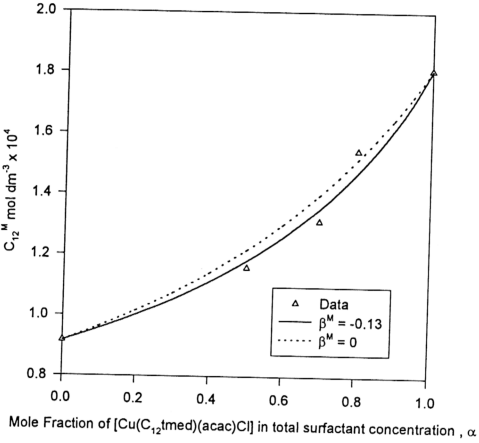

Figure 3-09 : C_{12}^{M} vs. mole fraction of [Cu(C_{12}tmed)(acac)Cl] in total surfactant concentration of mixed surfactant system with $C_{12}E_8$ as co-surfactant .

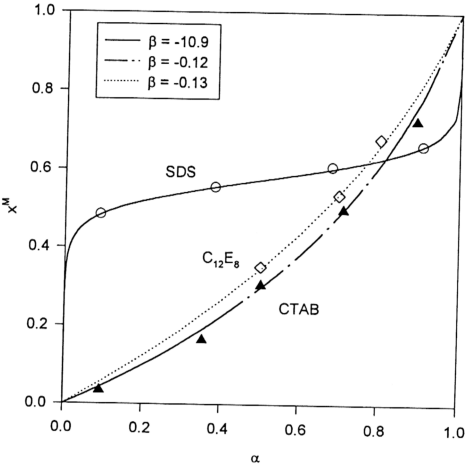

Figure 3-10 : Plot of micellar composition x^M against monomer composition α for binary surfactant system : (___) Cu / SDS , (__ .) Cu / CTAB and (.....) Cu / $C_{12}E_8$.

Monolayer interaction parameter , β^{σ} (Rosen's model)

For mixed monolayer , the nonideality is measured by monolayer interaction parameter , β^{σ} . Rosen and coworker extended the Regular Solution approach for the treatment of surfaces of aqueous solution of surfactant mixtures by considering the molar area properties of the surfactants [22(f)] .

Treatment "R" : It is based upon the assumption that the ratio of the partial molar areas of the surfactants in the mixed monolayer equals the ratio of the molar monolayer areas of the two individual surfactants , i.e.,

$$\frac{A_1}{A_2} = \frac{A_1^0}{A_2^0} \tag{3-10}$$

and

$$A_{av} = x^{\sigma} A_1 + \left(1 - x^{\sigma}\right) A_2 \tag{3-11}$$

$$\beta^{\sigma R} = \frac{\ln\left[\frac{\alpha C_{12}}{x^{\sigma R} C_1^0}\right] - \frac{\gamma A_1^0}{RT}\left[1 - \frac{A_{av}}{x^{\sigma R} A_1^0 + (1 - x^{\sigma R}) A_2^0}\right]}{\left(1 - x^{\sigma R}\right)^2} = \frac{\ln\left[\frac{(1-\alpha) C_{12}}{(1 - x^{\sigma R}) C_2^0}\right] - \frac{\gamma A_2^0}{RT}\left[1 - \frac{A_{av}}{x^{\sigma R} A_1^0 + (1 - x^{\sigma R}) A_2^0}\right]}{\left(x^{\sigma R}\right)^2} \tag{3-12}$$

Treatment "E" : It is based upon the assumption that the area occupied by the surfactant in the mixed monolayer is not significantly different from that in a monolayer of the individual surfactant , i.e. , $A_1 \approx A_1^0$ and $A_2 \approx A_2^0$

$$\beta^{\sigma E} = \frac{\ln\left[\frac{\alpha C_{12}}{x^{\sigma E} C_1^0}\right]}{\left(1 - x^{\sigma E}\right)^2} = \frac{\ln\left[\frac{(1-\alpha) C_{12}}{(1 - x^{\sigma E}) C_2^0}\right]}{\left(x^{\sigma E}\right)^2} \tag{3-13}$$

where

C_1^0, C_2^0, C_{12}^0 = Concentration of pure surfactants 1 , 2 and their mixture at certain surface tension value

α = mole fraction of surfactant 1 in the total mixed surfactant

x^σ = mole fraction of surfactant 1 in the mixed monolayer

β^σ = interaction parameter for the mixed monolayer

A_{av} = the average area per surfactant molecule in the mixed monolayer at the interface

A_1, A_2 = the partial molar interface areas occupied by surfactants 1 and 2 , respectively , at the mixed surfactant interface .

A_1^0, A_2^0 = the molar interface areas occupied by surfactants 1 and 2 , respectively , at the pure surfactant interface .

Values of interaction parameters $\beta^{\sigma,E}$ and $\beta^{\sigma,R}$ for mixture monolayer at given surface tension values for Cu(C_{12}tmed)(acac)Cl and co-surfactants SDS , CTAB and $C_{12}E_8$ are shown in Tables 3-05(a) , 3-05(b) , 3-07(a) , 3-07(b) , 3-09(a) and 3-09(b) ; the calculated monolayer mole fractions , $x^{\sigma E}$ and $x^{\sigma R}$, are shown in Tables 3-06(a) , 3-06(b) , 3-08(a) , 3-08(b) , 3-10(a) and 3-10(b) .

Table 3-05(a) : Interaction parameter $\beta^{\sigma,E}$ at various selected surface tension values for mixed monolayer of $Cu(C_{12}tmed)(acac)Cl$ and SDS

	$\beta^{\sigma,E}$					
α	γ = 41	γ = 43	γ = 45	γ = 47	γ = 49	γ = 51
0.09	-11.6	-11.2	-10.7	-10.3	-9.8	-9.4
0.38	-11.4	-11.0	-10.5	-10.0	-9.6	-9.1
0.68	-11.2	-10.8	-10.5	-10.1	-9.8	-9.4
0.91	-10.8	-10.4	-10.0	-9.6	-9.1	-8.7
Average	-11.3 ±0.3	-10.8 ±0.2	-10.4 ±0.2	-10.0 ±0.2	-9.6 ±0.2	-9.2 ±0.2

Table 3-05(b) : Interaction parameter $\beta^{\sigma,R}$ at various selected surface tension values for mixed monolayer of $Cu(C_{12}tmed)(acac)Cl$ and SDS

	$\beta^{\sigma,R}$					
α	γ = 41	γ = 43	γ = 45	γ = 47	γ = 49	γ = 51
0.09	-20.8	-20.7	-20.7	-20.7	-20.7	-20.7
0.38	-20.6	-20.6	-20.6	-20.6	-20.6	-20.6
0.68	-18.1	-18.1	-18.1	-18.1	-18.1	-18.1
0.91	-18.8	-18.8	-18.8	-18.8	-18.8	-18.8
Average	-19.6 ±1.1	-19.6 ±1.1	-19.6 ±1.1	-19.5 ±1.1	-19.5 ±1.1	-19.5 ±1.1

Table 3-06(a) : Surface mole fraction $x^{\sigma,E}$ at various selected surface tension values for mixed monolayer of $Cu(C_{12}tmed)(acac)Cl$ and SDS

	$x^{\sigma,E}$					
α	γ = 41	γ = 43	γ = 45	γ = 47	γ = 49	γ = 51
0.09	0.47	0.47	0.47	0.47	0.47	0.47
0.38	0.54	0.54	0.55	0.55	0.55	0.56
0.68	0.59	0.59	0.60	0.60	0.60	0.61
0.91	0.65	0.66	0.66	0.67	0.68	0.69

Table 3-06(b) : Surface mole fraction $x^{\sigma,R}$ at various selected surface tension values for mixed monolayer of $Cu(C_{12}tmed)(acac)Cl$ and SDS

	$x^{\sigma,R}$					
α	γ = 41	γ = 43	γ = 45	γ = 47	γ = 49	γ = 51
0.09	0.48	0.48	0.48	0.48	0.48	0.48
0.38	0.52	0.52	0.52	0.52	0.52	0.52
0.68	0.55	0.55	0.55	0.55	0.55	0.55
0.91	0.59	0.59	0.59	0.59	0.59	0.59

Table 3-07(a) : Interaction parameter $\beta^{\sigma,E}$ at various selected surface tension values for mixed monolayer of Cu(C_{12}tmed)(acac)Cl and CTAB

	$\beta^{\sigma,E}$					
α	γ = 45	γ = 47	γ = 49	γ = 51	γ = 53	γ = 55
0.09	-0.8_5	-0.7_6	-0.6_7	-0.5_6	-0.4_4	-0.3_1
0.35	-0.1_7	-0.1_0	-0.0_3	0.0_4	0.1_2	0.2_0
0.50	-0.1_3	-0.0_7	0	0.0_7	0.1_4	0.2_2
0.71	-0.2_1	-0.1_4	-0.0_6	0	0.0_8	0.1_5
0.89	-0.2_2	-0.1_6	-0.0_9	-0.0_2	0.0_5	0.1_2
Average	$-0.3_2 \pm 0.2_1$	$-0.2_4 \pm 0.2_1$	$-0.1_7 \pm 0.2_0$	$-0.0_9 \pm 0.1_9$	$0 \pm 0.1_7$	$0.0_8 \pm 0.1_5$

Table 3-07(b) : Interaction parameter $\beta^{\sigma,R}$ at various selected surface tension values for mixed monolayer of Cu(C_{12}tmed)(acac)Cl and CTAB

	$\beta^{\sigma,R}$					
α	γ = 45	γ = 47	γ = 49	γ = 51	γ = 53	γ = 55
0.09	-2.1	-2.1	-2.1	-2.1	-2.1	-2.1
0.35	-1.3	-1.3	-1.3	-1.3	-1.3	-1.3
0.50	-1.5	-1.5	-1.5	-1.5	-1.5	-1.5
0.71	-1.8	-1.8	-1.8	-1.8	-1.8	-1.8
0.89	-1.5	-1.5	-1.5	-1.5	-1.5	-1.5
Average	-1.6 ±0.3	-1.6 ±0.3	-1.6 ±0.3	-1.6 ±0.3	-1.6 ±0.3	-1.6 ±0.3

Table 3-08(a) : Surface mole fraction $x^{\sigma,E}$ at various selected surface tension values for mixed monolayer of Cu(C_{12}tmed)(acac)Cl and CTAB

	$x^{\sigma,E}$					
α	γ = 45	γ = 47	γ = 49	γ = 51	γ = 53	γ = 55
0.09	0.09	0.08	0.08	0.07	0.06	0.06
0.35	0.22	0.21	0.20	0.19	0.18	0.17
0.50	0.33	0.32	0.31	0.30	0.30	0.29
0.71	0.53	0.53	0.52	0.52	0.52	0.52
0.89	0.77	0.78	0.78	0.79	0.79	0.80

Table 3-08(b) : Surface mole fraction $x^{\sigma,R}$ at various selected surface tension values for mixed monolayer of Cu(C_{12}tmed)(acac)Cl and CTAB

	$x^{\sigma,R}$					
α	γ = 45	γ = 47	γ = 49	γ = 51	γ = 53	γ = 55
0.09	0.16	0.16	0.16	0.16	0.16	0.16
0.35	0.30	0.30	0.30	0.30	0.29	0.29
0.50	0.39	0.39	0.39	0.39	0.39	0.39
0.71	0.52	0.52	0.52	0.52	0.51	0.51
0.89	0.69	0.69	0.69	0.69	0.68	0.68

Table 3-09(a) : Interaction parameter $\beta^{\sigma,E}$ at various selected surface tension values mixed monolayer of $Cu(C_{12}tmed)(acac)Cl$ and $C_{12}E_8$

	$\beta^{\sigma,E}$			
α	γ = 40	γ = 42	γ = 44	γ = 46
0.50	-0.2_4	0	0.2_8	0.6_4
0.70	-0.2_5	-0.0_2	0.2_2	0.4_8
0.80	-0.3_1	-0.1_8	-0.0_5	0.0_8
Average	$-0.2_7 \pm 0.0_3$	$-0.0_7 \pm 0.0_8$	$0.1_5 \pm 0.1_4$	$0.4_0 \pm 0.2_1$

Table 3-09(b) : Interaction parameter $\beta^{\sigma,R}$ at various selected surface tension values for mixed monolayer of $Cu(C_{12}tmed)(acac)Cl$ and $C_{12}E_8$

	$\beta^{\sigma,R}$			
α	γ = 40	γ = 42	γ = 44	γ = 46
0.50	-3.2	-3.2	-3.2	-3.2
0.70	-4.2	-4.2	-4.2	-4.2
0.80	-2.6	-2.6	-2.6	-2.6
Average	-3.3 ±0.6	-3.3 ±0.6	-3.3 ±0.6	-3.3 ±0.6

Table 3-10(a) : Surface mole fraction $x^{\sigma,E}$ at various selected surface tension values for mixed monolayer of $Cu(C_{12}tmed)(acac)Cl$ and $C_{12}E_8$

	$x^{\sigma,E}$			
α	γ = 40	γ = 42	γ = 44	γ = 46
0.50	0.28	0.25	0.21	0.16
0.70	0.46	0.44	0.41	0.37
0.80	0.58	0.57	0.56	0.54

Table 3-10(b) : Surface mole fraction $x^{\sigma,R}$ at various selected surface tension values for mixed monolayer of $Cu(C_{12}tmed)(acac)Cl$ and $C_{12}E_8$

	$x^{\sigma,R}$			
α	γ = 40	γ = 42	γ = 44	γ = 46
0.50	0.42	0.41	0.41	0.40
0.70	0.51	0.50	0.50	0.49
0.80	0.56	0.55	0.54	0.54

In the mixed cationic-anionic surfactants , various factors that influence the value of monolayer interaction parameter , $\beta^{\sigma,E}$, had been studied by Goralczyk [95] . The absolute value of $\beta^{\sigma,E}$ decreases with the increase in surface tension (because the larger the distance between adsorbed ions, the smaller the adsorption, therefore the weaker the interactions) . The absolute value of $\beta^{\sigma,E}$ decreases with the increase in inorganic electrolyte concentration because rises in ionic strength of the solution will weaken the electrostatic interactions between the adsorbed ions . At constant inorganic electrolyte concentration the absolute value of $\beta^{\sigma,E}$ decreases in the order NaCl > NaBr > NaI (because the ability of inorganic anions to weaken the electrostatic interactions increases in the order $Cl^- < Br^- < I^-$) . By varying the chain length of anions and cations , Goralczyk found out that the interactions are essentially electrostatic in nature , while the interactions between the hydrophobic chains are much less important .

From the table above it can be seen that , $\beta^{\sigma,R}$ is always more negative than $\beta^{\sigma,E}$. Molecular interaction parameter values for mixed monolayer formation calculated by the "R" method , $\beta^{\sigma,R}$, are essentially constant with change in the interfacial tension , while values from the "E" method vary with interfacial tension .

Similar to that of the mixed micelle , the mixed monolayer formed from anionic-cationic surfactant is essentially close to the 1:1 ratio , i.e., equimolar surface composition is preferentially obtained . The monolayer mole fraction increases only slightly above 0.5 even though at high copper(II) concentration relative to that of SDS .

However for Cu / CTAB and Cu / $C_{12}E_8$ systems , the monolayer composition in Cu increases regularly with increasing concentration of Cu .

For both Cu / CTAB and Cu / $C_{12}E_8$ systems , again , $\beta^{\sigma,E}$ values vary with the surface tension values but $\beta^{\sigma,R}$ values are independent of surface tension . The result implies that the R-method , where the ratio of the partial molar areas of the surfactants in the mixed monolayer equals the ratio of the molar monolayer areas of the two individual surfactants , is a better method of estimating molecular interaction in the mixed monolayer . In marked contrast to that of Cu / SDS system , the mole fraction in the monolayer increases regularly with an increase in the mole fraction of Cu(II) surfactant in the total mixed surfactant .

Interaction of $Cu(C_{12}tmed)(acac)Cl$ with SDS is stronger in the mixed monolayer as compared to mixed micelle , as the β^{σ} value is more negative than β^{M} . β^{σ} is small for mixed monolayer of $Cu(C_{12}tmed)(acac)Cl$ - CTAB and $Cu(C_{12}tmed)(acac)Cl$ - $C_{12}E_8$ systems implying that their interaction is weak .

Synergism

Rosen and coworker had derived theoretical equations for the existence of synergism [22(b)].

Synergism is defined as the condition when the properties of the mixture are better than those attainable with the individual components by themselves .

Synergism in surface tension reduction efficiency exists when the total concentration of mixed surfactant required to reduce the surface tension of the solvent to a given value is less than that of either surfactant .

Synergism in surface tension reduction effectiveness exists when an aqueous binary mixture of surfactants at its CMC reaches a surface tension value lower than that attained at the CMCs of the individual surfactants .

The conditions for the existence of synergism for these 3 phenomena are :

1) surface tension reduction efficiency :

$$\beta^{\sigma} < 0 \tag{3-14}$$

$$\left|\beta^{\sigma}\right| > \left|\ln\left(\frac{C_1^0}{C_2^0}\right)\right| \tag{3-15}$$

2) mixed micelle formation :

$$\beta^{M} < 0 \tag{3-16}$$

$$\left|\beta^{M}\right| > \left|\ln\left(\frac{C_1^M}{C_2^M}\right)\right| \tag{3-17}$$

3) surface tension reduction effectiveness :

$$\beta^{\sigma} < 0 \tag{3-18}$$

$$\beta^{\sigma} - \beta^{M} < 0 \tag{3-19}$$

$$\left|\beta^{\sigma} - \beta^{M}\right| > \left|\ln\left(\frac{C_1^0}{C_2^0}\frac{C_2^M}{C_1^M}\right)\right| \tag{3-20}$$

where

C_i^0 = molar concentration of surfactant i at a given surface tension value

C_i^M = critical micelle concentration of surfactant i

The degree of synergism possible in mixed micelle formation in a mixture is measured by the maximum decrease in the CMC of the two individual surfactants composing the mixture ; i.e. , $\frac{\left(C_1^M - C_{12,\min}^M\right)}{C_1^M}$ or $1 - \frac{C_{12,\min}^M}{C_1^M}$ where $C_{12,\min}^M$ is the lowest possible CMC of the mixed surfactant system and C_1^M is the lower CMC of the two individual surfactants .

$$\frac{C_{12,\min}^M}{C_1^M} = \exp\left[\frac{\left(\beta^M - \ln\left(\frac{C_1^M}{C_2^M}\right)\right)^2}{4\beta^M}\right] \tag{3-21}$$

The greater the value of $1 - \frac{C_{12,\min}^M}{C_1^M}$ (maximum = 1) , the greater the degree of synergism .

The degree of synergism possible in surface tension reduction efficiency is measured by $\frac{\left(C_1^0 - C_{12,\min}\right)}{C_1^0}$ or $1 - \frac{C_{12,\min}}{C_1^0}$ where $C_{12,\min}$ is the minimum total mixed surfactant concentration required to attain a given surface tension .

$$\frac{C_{12,\min}}{C_1^0} = \exp\left[\frac{\left(\beta^\sigma - \ln\left(\frac{C_1^\sigma}{C_2^\sigma}\right)\right)^2}{4\beta^\sigma}\right] \qquad (3\text{-}22)$$

The greater the value of $1-\frac{C_{12,\min}}{C_1^0}$ (maximum = 1) , the greater the degree of synergism .

At the point of maximum synergism in mixed micelle formation , the mole fraction is given by

$$\alpha^{M*} = x^{M*} = \frac{\ln\left(\frac{C_1^M}{C_2^M}\right) + \beta^M}{2\beta^M} \qquad (3\text{-}23)$$

At the point of maximum synergism in mixed monolayer formation , the mole fraction is given by

$$\alpha^{\sigma*} = x^{\sigma*} = \frac{\ln\left(\frac{C_1^0}{C_2^0}\right) + \beta^\sigma}{2\beta^\sigma} \qquad (3\text{-}24)$$

Table 3-11 summarizes β^M , β^σ, $\beta^M - \beta^\sigma$ values obtained from Rubingh's equation (for mixed micelle) and Rosen's "R" method (for mixed monolayer) . Table 3-12 summarizes the magnitude of logarithm of ratio of C_i^0 and C_i^M from individual surfactant i . From Tables 3-11 and 3-12 , it is apparent that all the systems studied (Cu / SDS ; Cu / CTAB and Cu / $C_{12}E_8$), show synergism in surface tension reduction efficiency , as both conditions , $\beta^\sigma < 0$ and $|\beta^\sigma| > \left|\ln\left(\frac{C_1^0}{C_2^0}\right)\right|$, are obeyed .

In the case of mixed micelle formation , only Cu / SDS system shows synergism in mixed micelle formation where both conditions $\beta^M < 0$ and $|\beta^M| > \left|\ln\left(\frac{C_1^M}{C_2^M}\right)\right|$ are achieved . For the other two systems (CTAB and $C_{12}E_8$), their β^M are much smaller than $\ln\left(\frac{C_1^M}{C_2^M}\right)$ values ; therefore , no synergism occurs .

Both Cu / SDS and Cu / $C_{12}E_8$ systems show synergism in surface tension reduction effectiveness , as both obey the conditions of $\beta^\sigma < 0$, $\beta^\sigma - \beta^M < 0$ and $|\beta^\sigma - \beta^M| > \left|\ln\left(\frac{C_1^0}{C_2^0}\frac{C_2^M}{C_1^M}\right)\right|$. In Cu / CTAB system , no synergism occurs in surface tension reduction effectiveness .

The degrees of synergism in surface tension reduction efficiency and in mixed micelle formation are summarized in Table 3-13 . Cu / SDS system achieves greater degree of synergism in both cases as the $1-\frac{C_{12,\min}^M}{C_1^M}$ and $1-\frac{C_{12,\min}}{C_1^0}$ values approach 1 . Although both Cu / CTAB and Cu / $C_{12}E_8$ systems do not fulfill the condition of synergism in mixed micelle formation , the degree of synergism is also listed in Table 3-13 . Their $1-\frac{C_{12,\min}^M}{C_1^M}$ values are much lower when compared to Cu / SDS system . $1-\frac{C_{12,\min}}{C_1^0}$ in Cu / $C_{12}E_8$ system (0.31) is higher than Cu / CTAB system (0.10) because molecular interaction of Cu / $C_{12}E_8$ (β^σ = -3.3) is stronger than Cu / CTAB (β^σ = -1.6) .

Mole fractions at the maximum synergism in the mixed micelle x^{M^*} , in mixed monolayer x^{σ^*} and the calculated $C_{12,\min}^{M}$ and $C_{12,\min}$ values for the mixed surfactant systems are shown in Table 3-14 .

Table 3-11 : Micellar and monolayer interaction parameters β^M , β^σ , $\beta^\sigma - \beta^M$ for the mixed surfactant system

System	T (°C)	β^M	β^σ	$\beta^\sigma - \beta^M$
$Cu(C_{12}tmed)(acac)Cl$ + SDS	20	-10.9	-19.6	-8.7
$Cu(C_{12}tmed)(acac)Cl$ + CTAB	22	-0.12	-1.6	-1.5
$Cu(C_{12}tmed)(acac)Cl$ + $C_{12}E_8$	22	-0.13	-3.3	-3.2

Table 3-12 : Magnitude of logarithm of ratio of concentrations in mixed surfactant system

System	$\left\lvert \ln\left(\frac{C_1^M}{C_2^M}\right)\right\rvert$	$\left\lvert \ln\left(\frac{C_1^0}{C_2^0}\right)\right\rvert$	$\left\lvert \ln\left(\frac{C_1^0}{C_2^0}\frac{C_2^M}{C_1^M}\right)\right\rvert$
$Cu(C_{12}tmed)(acac)Cl$ + SDS	1.9	$1.6_5^{(1)} \pm 0.0_4$	$3.5_2^{(1)} \pm 0.0_4$
$Cu(C_{12}tmed)(acac)Cl$ + CTAB	0.9	$0.8_0^{(2)} \pm 0.0_1$	$1.7_1^{(2)} \pm 0.0_1$
$Cu(C_{12}tmed)(acac)Cl$ + $C_{12}E_8$	0.7	$1.1_3^{(3)} \pm 0.1_0$	$1.8_1^{(3)} \pm 0.1_0$

C_1^0 , C_2^0 = molar concentrations of individual surfactants 1 and 2 , respectively , required to yield a given surface tension value .

(1) Average value at given γ of 41 , 43 , 45 , 47 , 49 , 51 mN m^{-1}

(2) Average value at given γ of 45 , 47 , 49 , 51 , 53 , 55 mN m^{-1}

(3) Average value at given γ of 40 , 42 , 44 , 46 mN m^{-1}

Table 3-13 : Degree of synergism in surface tension reduction efficiency and in mixed micelle formation

System	$1-\frac{C_{12,min}^{M}}{C_{1}^{M}}$	$1-\frac{C_{12,min}}{C_{1}^{0}}$
$Cu(C_{12}tmed)(acac)Cl$ + SDS	0.97_6	0.99_7
$Cu(C_{12}tmed)(acac)Cl$ + CTAB	0.73	0.10
$Cu(C_{12}tmed)(acac)Cl$ + $C_{12}E_8$	0.43	0.30

Table 3-14 : Mole fractions at the maximum synergism in mixed micelle , in mixed monolayer and the calculated $C_{12,min}^{M}$ and $C_{12,min}$ values

System	x^{M*}	$x^{\sigma*}$	$C_{12,min}^{M}$	$C_{12,min}$
$Cu(C_{12}tmed)(acac)Cl$ + SDS	0.41	0.46	4.3×10^{-6}	3.4×10^{-7} [4]
$Cu(C_{12}tmed)(acac)Cl$ + CTAB	-	0.75	4.8×10^{-5}	5.4×10^{-5} [5]
$Cu(C_{12}tmed)(acac)Cl$ + $C_{12}E_8$	-	0.67	1.0×10^{-4}	8.6×10^{-5} [6]

[4] Value at given $\gamma = 45$ mN m^{-1}
[5] Value at given $\gamma = 49$ mN m^{-1}
[6] Value at given $\gamma = 42$ mN m^{-1}

Surface interaction parameter , β^S (Holland's model)

Holland [20(c),20(d)] developed nonideal analog of Butler's equation to treat the nonideality at interfaces of mixed surfactant solutions . This approach requires micellar interaction parameter β^M and micellar mole fraction x^M calculated from Rubingh's equation . Based on the assumption of $A_i = A_i^0$, the nonideality measured by surface interaction parameter β^S is given as

$$\beta^S = \frac{1}{\left(1-x^S\right)^2} \ln\left[\frac{x^M \exp\left[\beta^M\left(1-x^M\right)^2\right]}{x^S \exp\left[\frac{A_1^0}{RT}\left(\pi-\pi_1^{max}\right)\right]}\right] = \frac{1}{\left(x^S\right)^2} \ln\left[\frac{\left(1-x^M\right)\exp\left[\beta^M\left(x^M\right)^2\right]}{\left(1-x^S\right)\exp\left[\frac{A_2^0}{RT}\left(\pi-\pi_2^{max}\right)\right]}\right] \qquad (3\text{-}25)$$

where

π = surface pressure in mixed system

π_i^{max} = surface pressure of surfactant component i at or above CMC in pure system

A_i^o = area per mole of surfactant i in pure system

A_i = area per mole of surfactant i in mixed system

β^S , β^M = surface , micellar interaction parameter

x^S , x^M = surface and micellar mole fraction of surfactant 1 in the mixed monolayer / mixed micelle system

The calculated surface interaction parameter and surface mole fraction for mixed Cu / SDS , Cu / CTAB and Cu / $C_{12}E_8$ systems are shown in Tables 3-15(a) to 3-15(c) . Surface tensions at the CMC for binary mixtures of Cu / SDS , Cu / CTAB and Cu / $C_{12}E_8$

systems in 0.1 M NaCl versus mole fraction of Cu are shown in Figures 3-11 to 3-13 , with error bar 0.2 $mN\,m^{-1}$ indicated . The solid lines are the prediction from the nonideal monolayer mixing model , and the dashed line the prediction based on ideal mixing .

The nonideal interaction parameter for surface mixing (β^S = -13.1) is more negative than in the micellar pseudophase (β^M = -10.9) , suggesting possible synergism in surface tension behavior . The parameter β^S is able to account empirically for effects due to changes in molar areas on mixing in binary systems .

For Cu / $C_{12}E_8$ binary mixtures , the data fit Holland's model quite well , the surface tensions at the CMC are in good agreement with the nonideal model . For the Cu / SDS system , Holland's model predicts a sharp drop in surface tension at the both ends and level off in between these two ends , but the experiment gives surface tension minimum when the mixing ratio approaches 1 : 1 .

Holland's model fails to fit the surface tension value in Cu / CTAB case . One reason that may account for this failure is that the surface tension range is too narrow within the mixing ratio (from 38.5 to 40 $mN\,m^{-1}$) and there is difficulty in determining very accurate surface tension value .

In order to test and verify this model , a separate experiment to measure accurately the surface tension has to be done . The surface tension above the CMC for various mixing ratio should be measured on the same day , instead of different days under different environments , because although the precision of the surface tension data is $\pm$ 0.2 $mN\,m^{-1}$, the same solution measured in different days may deviate from each other by as much as $\pm$ 0.5 $mN\,m^{-1}$.

Table 3-15(a) : Surface mole fraction and interaction parameter for mixed surfactant system $Cu(C_{12}tmed)(acac)Cl$ and SDS based on $\beta^M = -10.9$

α	β^s	x^s
0.09	-13.0	0.47
0.38	-14.1	0.53
0.68	-13.3	0.57
0.91	-12.0	0.64
Average	$-13.1 \pm 0.6^*$	-

Table 3-15(b) : Surface mole fraction and interaction parameter for mixed surfactant system $Cu(C_{12}tmed)(acac)Cl$ and CTAB based on $\beta^M = -0.12$

α	β^s	x^s
0.09	-1.2_0	0.11
0.35	-0.5_9	0.26
0.50	-0.2_5	0.34
0.71	-0.3_5	0.53
0.89	0.0_6	0.80
Average	$-0.4_7 \pm 0.3_5$	-

Table 3-15(c) : Surface mole fraction and interaction parameter for mixed surfactant system $Cu(C_{12}tmed)(acac)Cl$ and $C_{12}E_8$ based on $\beta^M = -0.13$

α	β^s	x^s
0.50	-0.5_3	0.33
0.70	-0.5_9	0.48
0.80	-0.7_2	0.59
Average	$-0.5_8 \pm 0.0_9$	-

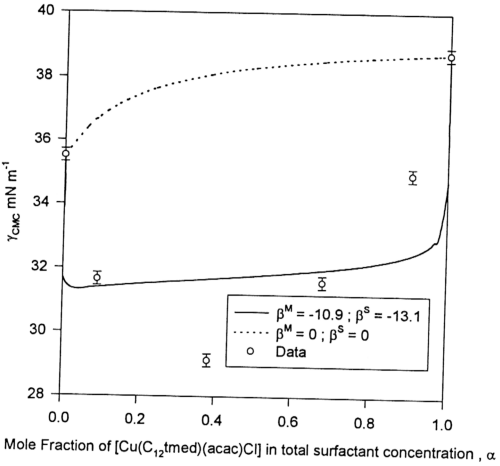

Figure 3-11 : Surface tension at the CMC for binary mixtures of Cu / SDS system

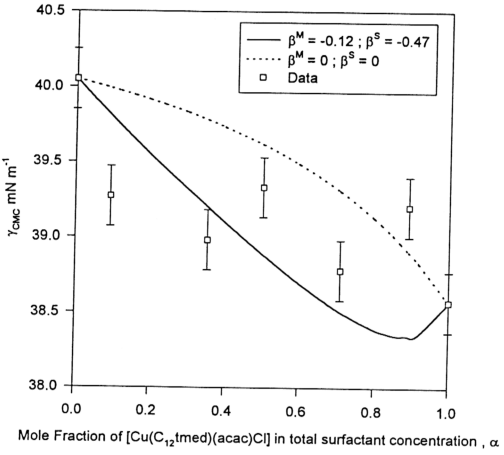

Figure 3-12 : Surface tension at the CMC for binary mixtures of Cu / CTAB system

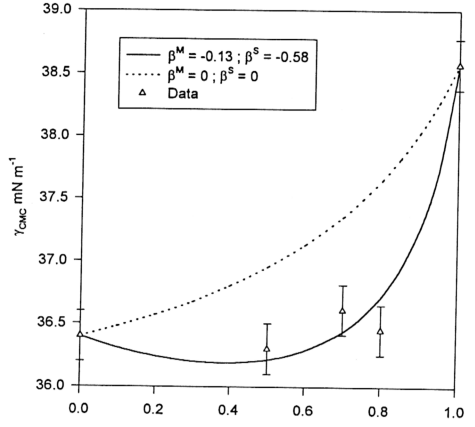

Figure 3-13 : Surface tension at the CMC for binary mixtures of Cu / $C_{12}E_8$ system

(II) Gibbs-Duhem equation : (a) Motomura's approach

Motomura [30] derived equation to estimate the micellar composition based on thermodynamic consideration . The composition of the mixed micelle formed by surfactants 1 and 2 is derived using the relationship

$$\overline{x_2^M} = \overline{\alpha_2} - n\left(\frac{\overline{\alpha_1 \alpha_2}}{C_{12}^M}\right)\left(\frac{\partial \overline{C_{12}^M}}{\partial \alpha_2}\right)_{T,P} \qquad (3\text{-}26)$$

where

$$n = \frac{\nu_{1,c}\nu_2\overline{\alpha_1} + \nu_{2,d}\nu_1\overline{\alpha_2}}{\nu_{1,c}\nu_2\overline{\alpha_1} + \nu_{2,d}\nu_1\overline{\alpha_2} - \delta_d^c\nu_{1,c}\nu_{2,d}} \qquad (3\text{-}27)$$

$$\overline{C_{12}^M} = (\nu_1\alpha_1 + \nu_2\alpha_2)C_{12}^M \qquad (3\text{-}28)$$

$$\overline{\alpha_i} = \frac{\nu_i\alpha_i}{\nu_1\alpha_1 + \nu_2\alpha_2} \qquad (3\text{-}29)$$

Here , surfactant 1 dissociates to give $\nu_{1,a}$ anion and $\nu_{1,c}$ cation , surfactant 2 dissociates to give $\nu_{2,b}$ anion and $\nu_{2,d}$ cation . ν_i is the number of ions contributed by a surfactant i and δ_d^c is the Kronecker delta defined by $\delta_d^c = 0$ when $d \neq c$ and $\delta_d^c = 1$ when $d = c$.

Since Cu(C_{12}tmed)(acac)Cl , SDS , CTAB are 1 : 1 type of ions , therefore in Cu / SDS and Cu / CTAB systems , $\nu_{1,a} = \nu_{1,c} = \nu_{2,b} = \nu_{2,d} = 1$. For $C_{12}E_8$, since there is no counterion , $\nu_{1,c} = 0$. Surfactant 2 in binary mixtures is referred to Cu(C_{12}tmed)(acac)Cl . The values that are used in equation 3-26 are shown in Tables 3-16 and 3-17 . For both Cu

/ SDS and Cu / CTAB systems , $\overline{\alpha_2} = \alpha_2$, $\overline{C_{12}^M} = 2C_{12}^M$ and $n = 1$. For Cu / $C_{12}E_8$ system $\overline{\alpha_2} = \frac{2\alpha_2}{\alpha_1 + 2\alpha_2}$, $\overline{C_{12}^M} = (\alpha_1 + 2\alpha_2)C_{12}^M$ and $n = 1$.

Data of $\overline{C_{12}^M}$ versus $\overline{\alpha_2}$ are fitted with reciprocal quadratic equation , $\overline{C_{12}^M} = \frac{1}{a + b(\overline{\alpha_2}) + c(\overline{\alpha_2})^2}$, where a , b and c are the constant . The values of a , b and c are shown in Table 3-18 . Differentiation of the reciprocal quadratic equation produces $\frac{\partial \overline{C_{12}^M}}{\partial \overline{\alpha_2}} = \frac{-[b + 2c(\overline{\alpha_2})]}{[a + b(\overline{\alpha_2}) + c(\overline{\alpha_2})^2]^2}$ values , which are substituted into equation 3-26 to give $\overline{x_2^M}$.

Plots of CMC of mixtures $\overline{C_{12}^M}$ versus mole fraction of Cu in total surfactant concentrations $\overline{\alpha_2}$ and in mixed micelle $\overline{x_2^M}$ of binary mixtures are shown in Figures 3-14 to 3-16 .

Cu / SDS system deviates from the ideality in such a way that the $\overline{C_{12}^M}$ versus $\overline{\alpha_2}$ and $\overline{C_{12}^M}$ versus $\overline{x_2^M}$ curves have a common minimum point at which they coincide . $\overline{C_{12}^M}$ decreases along a curve from both ends to a minimum point in the middle . $\overline{x_2^M}$ is smaller than $\overline{\alpha_2}$ at higher composition (right of minimum point) and larger at a lower composition (left of minimum point) . To the left of the minimum , Cu is richer in the micellar phase

($\overline{x_2^M}$) than in monomer phase ($\overline{\alpha_2}$). To the right of the minimum , just the opposite is true . At the minimum point , called the azeotrope , the monomer ($\overline{\alpha_2}$) and micellar ($\overline{x_2^M}$) phases have the same composition . These systems exhibit negative deviations from ideal behavior , that is $f_i^M < 1$ and the excess Gibbs free energy is negative [83] . Since the azeotropy is closely related to the interaction between the constituent molecules in the system , the nonideal behavior may be accounted for apparently by the stronger molecular interaction between Cu and SDS [30].

The shape formed by $\overline{C_{12}^M}$ versus $\overline{\alpha_2}$ and $\overline{C_{12}^M}$ versus $\overline{x_2^M}$ curves in Cu / CTAB and Cu / $C_{12}E_8$ system are seen to form a bow shape . $\overline{C_{12}^M}$ values are intermediate between those of the pure components , $\overline{C_1^M}$ and $\overline{C_2^M}$. The micellar state ($\overline{x_2^M}$) in such systems is always smaller than the monomer state ($\overline{\alpha_2}$) over the entire range of composition . This suggests that both Cu and CTAB (also Cu and $C_{12}E_8$) mix ideally in the micellar state . This is proven by micellar interaction parameter approaching zero for both systems with β^M = -0.12 (Cu / CTAB) and β^M = -0.13 . The bow shape in Cu / $C_{12}E_8$ curves appears to be slightly thicker than Cu / CTAB because β^M is slightly more negative .

Table 3-16 : $\nu_{1,a}$, $\nu_{1,c}$, $\nu_{2,b}$, $\nu_{2,d}$, ν_1 , ν_2 and δ_d^c values from dissociation of surfactant 1 and 2

Surfactant		$\nu_{1,a}$	$\nu_{1,c}$	$\nu_{2,b}$	$\nu_{2,d}$	ν_1	ν_2	δ_d^c
1	2							
SDS	Cu	1	1	1	1	2	2	0
CTAB	Cu	1	1	1	1	2	2	0
$C_{12}E_8$	Cu	1	0	1	1	1	2	0

Table 3-17 : Calculated $\overline{\alpha_1}$, $\overline{\alpha_2}$, $\overline{C_{12}^M}$ and n values based on ν_1 , ν_2 values from Table 3-16

Surfactant		$\overline{\alpha_1}$	$\overline{\alpha_2}$	$\overline{C_{12}^M}$	n
1	2				
SDS	Cu	α_1	α_2	$2C_{12}^M$	1
CTAB	Cu	α_1	α_2	$2C_{12}^M$	1
$C_{12}E_8$	Cu	$\frac{\alpha_1}{\alpha_1+2\alpha_2}$	$\frac{2\alpha_2}{\alpha_1+2\alpha_2}$	$(\alpha_1+2\alpha_1)C_{12}^M$	1

Table 3-18 : Parameter a, b and c in quadratic equation $\overline{C_{12}^{M}} = \dfrac{1}{a + b\left(\overline{\alpha_2}\right) + c\left(\overline{\alpha_2}\right)^2}$

that are used to fit the $\overline{C_{12}^{M}}$ versus $\overline{\alpha_2}$ data for Cu / SDS , Cu / CTAB and Cu / $C_{12}E_8$ systems

System	a	b	c	ρ
Cu(C_{12}tmed)(acac)Cl + SDS *	8843	2732	-24972	0.9903
Cu(C_{12}tmed)(acac)Cl + CTAB	6599	-2375	-1402	0.9932
Cu(C_{12}tmed)(acac)Cl + $C_{12}E_8$	10842	-6953	-1148	0.9978

* The equation was used to fit data from $\alpha = 0.1$ to 0.9 in Cu / SDS case ρ = Correlation coefficient .

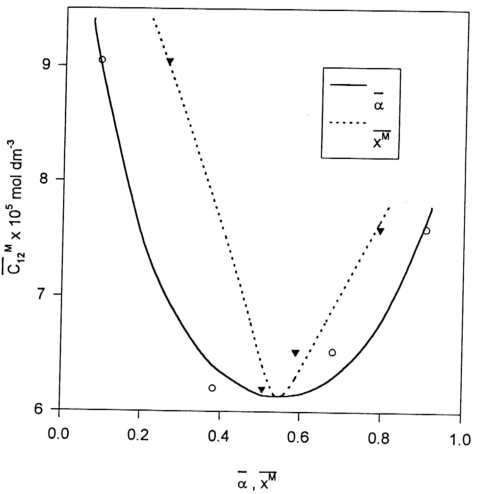

Figure 3-14 : $\overline{C_{12}^{M}}$ vs. $\overline{\alpha_2}$ and $\overline{C_{12}^{M}}$ vs. $\overline{x_2^{M}}$ curves for binary mixtures of Cu / SDS system

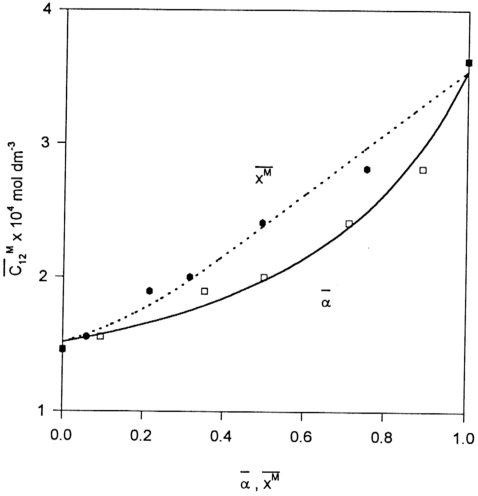

Figure 3-15 : $\overline{C_{12}^{M}}$ vs. $\overline{\alpha_2}$ and $\overline{C_{12}^{M}}$ vs. $\overline{x_2^{M}}$ curves for binary mixtures of Cu / CTAB system

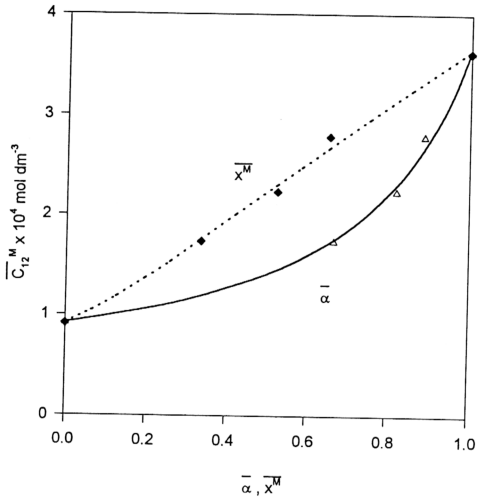

Figure 3-16 : $\overline{C_{12}^{M}}$ vs. $\overline{\alpha_2}$ and $\overline{C_{12}^{M}}$ vs. $\overline{x_2^{M}}$ curves for binary mixtures of Cu / $C_{12}E_8$ system

(II) Gibbs-Duhem equation : (b) Scamehorn's approach

Scamehorn, et. al. [29(a)] applied Gibbs-Duhem equation and pseudophase model to determine monomer-micelle equilibrium compositions . The mole fraction of surfactant 1 in the mixed micelle x^M is calculated from the slope of $\ln C_{12}^M$ versus α :

$$x^M = \alpha\left[1-(1-\alpha)\left(\frac{d\ln C_{12}^M}{d\alpha}\right)\right] \qquad (3\text{-}30)$$

The activity coefficient of surfactants in micelle can be calculated from the following equations :

$$f_1^M = \frac{\alpha C_{12}^M}{x^M C_1^M} \qquad (3\text{-}31)$$

$$f_2^M = \frac{(1-\alpha)C_{12}^M}{(1-x^M)C_2^M} \qquad (3\text{-}32)$$

This approach applies only to binary surfactant systems containing swamping electrolyte .

The plots of $\ln C_{12}^M$ versus α are shown in Figure 3-17 . The data of $\ln C_{12}^M$ versus α are curve fitted with quadratic equation $\ln C_{12}^M = a + b\alpha + c\alpha^2$ with a, b and c as constant . The values of a, b and c in quadratic equation are tabulated in Table 3-19 . The quadratic equation is further differentiated to give $\frac{d\ln C_{12}^M}{d\alpha} = b + 2c\alpha$ which was then substituted into equation 3-30 to produce x^M values . The calculated x^M values based on equation 3-30 for binary mixtures Cu / SDS , Cu / CTAB and Cu / $C_{12}E_8$ systems are plotted against f_1^M and f_2^M in Figures 3-18 to 3-20.

(II) Gibbs-Duhem equation : (c) Yu's approach

Yu, Z.-J. et. al. [41] deduced micellar composition by Gibbs-Duhem approach without using any CMC information of the pure surfactant systems . The molar ratio is given by :

$$\frac{n_1^M}{n_2^M} = -\frac{d\ln C_{2m}}{d\ln C_{1m}} \qquad (3\text{-}33)$$

where

C_{im} = concentration of species i in the solvent phase .

Using $x^M = \frac{n_1^M}{n_1^M + n_2^M}$, it can be easily shown that the mole fraction of surfactant 1 in the mixed micelles x^M can be related to molar ratio $\frac{n_1^M}{n_2^M}$ by the following equation :

$$x^M = \frac{1}{1 + \frac{1}{\left(\frac{n_1^M}{n_2^M}\right)}} \qquad (3\text{-}34)$$

Similarly x^M obtained from the Regular Solution approach can be converted to $\frac{n_1^M}{n_2^M}$.

The plots of $\ln C_{2m}$ versus $\ln C_{1m}$ are shown in Figure 3-21 . Data of $\ln C_{2m}$ versus $\ln C_{1m}$ were fitted with suitable equation , such as quadratic equation $\ln C_{2m} = a + b(C_{1m}) + c(C_{1m})^2$. Table 3-20 shows values of parameter that were used

to fit the data . The equation was then differentiated to give the gradient $\frac{d \ln C_{2m}}{d \ln C_{1m}}$.

The mole fraction of surfactant 1 in the mixed micelle , x^M , can be obtained from equation 3-34 . The calculated x^M values are plotted against ratio $\frac{[Cu]}{[Cosurfactant]}$ in Figures 3-22 to 3-24 for Cu / SDS , Cu / CTAB and Cu / $C_{12}E_8$ binary mixtures .

Comparison of micellar mole fraction x^M calculated from Motomura , Scamehorn and Yu's methods :

As the three groups applied Gibbs-Duhem equation (where extra parameter is not necessary) to calculate the micellar mole fraction , it is therefore necessary to compare their methods and find out which is more preferable .

x^M calculated from Motomura , Scamehorn and Yu's methods are plotted against ratio $\frac{[Cu]}{[Cosurfactant]}$ in Figures 3-22 to 3-24 for Cu / SDS , Cu / CTAB and Cu / $C_{12}E_8$ binary mixtures . x^M versus α are also tabulated in Tables 3-21(a) to 3-21(c) . The x^M values calculated from Rubingh's method are also included for the purpose of comparison .

In Cu / SDS system , (Figure 3-22) , initially , the micellar mole fraction x^M increases rapidly with a low Cu content in the mixed surfactant and start to level off at [Cu] / [SDS] ≈ 1 to give $x^M = 0.65$. This implies that the mixed micelle is mainly composed of nearly equimolar ratio of each component in a wide composition range of the mixed solutions .

In Figure 3-23 (Cu / CTAB mixture) , x^M increases gradually with increasing ratio of [Cu] / [CTAB] . Similarly for Cu / $C_{12}E_8$, where x^M increases steadily with increasing ratio of [Cu] / [$C_{12}E_8$] (Figure 3-24) .

In all the binary mixtures , both Motomura and Scamehorn give similar trend and the curves almost overlap ; this can be expected since the equation are quite similar , except for the definitions of $\overline{\alpha_2}$ and $\overline{C_{12}^M}$ in Motomura case . Yu's approach also gives similar plots in [Cu] / [SDS] and [Cu] / [CTAB] mixtures , except for [Cu] / [$C_{12}E_8$] binary mixture .

Therefore , overall , we can conclude that the three approaches which are based on the Gibbs-Duhem equation give similar results in binary surfactant mixtures .

Azeotropic behavior

Mixed cationic-anionic micelles of Cu / SDS deviate greatly from ideality with nonideal micellar parameter $\beta^M = -10.9$. The deviation causes the mixture CMC to be less than those of the pure components , resulting in a minimum in mixture CMC as a function of monomer composition . According to Osborne-Lee [28] , the existence of a minimum in the mixture CMC is consistent with the existence of an azeotropic composition in which the mole fractions of Cu surfactant in the monomer and micellar pseudophase are identical ($\alpha = x_1^M$) . The mixture CMC is given by

$$C_{12}^M = f_1^M x_1^M C_1^M + f_2^M x_2^M C_2^M \qquad (3\text{-}35)$$

Differentiating C_{12}^M over x_1^M gives

$$\frac{dC_{12}^M}{dx_1^M} = \left(f_1^M C_1^M - f_2^M C_2^M\right) + \left(x_1^M C_1^M \frac{df_1^M}{dx_1^M} + x_2^M C_2^M \frac{df_2^M}{dx_1^M}\right)$$

(3-36)

Since

$$x_1^M f_1^M C_1^M = \alpha_1 C_{12}^M \tag{3-37}$$

and

$$x_2^M f_2^M C_2^M = \alpha_2 C_{12}^M \tag{3-38}$$

for an azeotrope ($\alpha_1 = x_1^M$, $\alpha_2 = x_2^M$) , equation 3-36 reduces to

$$\frac{dC_{12}^M}{dx_1^M} = \left(x_1^M \frac{d \ln f_1^M}{dx_1^M} + x_2^M \frac{d \ln f_2^M}{dx_1^M} \right) C_{12}^M \tag{3-39}$$

In a two-component system , when the variation of activity coefficient with mole fraction for one of the components is known , the variation for the other component can be obtained from [83]

$$x_1^M \frac{d \ln f_1^M}{dx_1^M} = -x_2^M \frac{d \ln f_2^M}{dx_1^M} = x_2^M \frac{d \ln f_2^M}{dx_2^M} \tag{3-40}$$

Substituting equation 3-40 into 3-39 gives

$$\frac{dC_{12}^M}{dx_1^M} = 0 \tag{3-41}$$

The expression at the right hand side of equation 3-39 vanishes upon application of the Gibbs-Duhem equation . Thus when $\alpha_1 = x_1^M$, the mixture CMC must exhibit an extremum (maximum or minimum) .

Figure 3-25 (for Cu / SDS system) shows the calculated micellar compositions plotted against monomer compositions based on Scamehorn approach . As shown in Figure 3-26, there is an azeotropic composition corresponding to the measured mixture CMC minima , similar to Figure 3-14 which is obtained based on Motomura's approach .

Table 3-19 : Parameters a, b and c in quadratic equation $\ln C_{12}^{M} = a + b\alpha + c\alpha^2$ that are used to fit the $\ln C_{12}^{M}$ versus α data in the Scamehorn's method

System	a	b	c	ρ
Cu(C_{12}tmed)(acac)Cl + SDS *	-9.83	-1.98	1.77	0.9984
Cu(C_{12}tmed)(acac)Cl + CTAB **	-9.52	0.60	0.14	0.9978
Cu(C_{12}tmed)(acac)Cl + $C_{12}E_8$	-9.30	0.25	0.45	0.9955

* The equation was used to fit data from α = 0.09 to 0.91 in Cu / SDS case

** The equation was used to fit data from α = 0 to 0.89 in Cu / CTAB case

Table 3-20 : Parameters a, b and c and equations that are used to fit the $\ln C_{2m}$ versus $\ln C_{1m}$ data in the Yu's method

System and Equation	a	b	c	ρ
Cu(C_{12}tmed)(acac)Cl + SDS $\ln C_{2m} = a + b(\ln C_{1m}) + c(\ln C_{1m})^2$	-89.1	-12.7	-0.51	0.9932
Cu(C_{12}tmed)(acac)Cl + CTAB $\ln C_{2m} = \ln\left(a + b(\ln C_{1m})^2 + c\exp(\ln C_{1m})\right)$	8.14×10^{-5}	-4.96×10^{-8}	-0.50	0.9988
Cu(C_{12}tmed)(acac)Cl + $C_{12}E_8$ $\ln C_{2m} = a + b(\ln C_{1m}) + c(\ln C_{1m})^2$	-31.1	-3.65	-0.15	0.9998

Table 3-21(a) : x^M calculated from Motomura , Scamehorn , Yu and Rubingh's methods for Cu / SDS system

α	x^M (Motomura)	x^M (Scamehorn)	x^M (Yu)	x^M (Rubingh)
0.09	0.26	0.23	0.07	0.48
0.38	0.51	0.53	0.53	0.55
0.68	0.59	0.59	0.65	0.60
0.91	0.79	0.80	0.68	0.66

Table 3-21(b) : x^M calculated from Motomura , Scamehorn , Yu and Rubingh's methods for Cu / CTAB system

α	x^M (Motomura)	x^M (Scamehorn)	x^M (Yu)	x^M (Rubingh)
0.09	0.06	0.04	0.03	0.11
0.35	0.22	0.19	0.21	0.26
0.50	0.31	0.32	0.32	0.34
0.71	0.50	0.55	0.54	0.53
0.89	0.75	0.81	0.80	0.80

Table 3-21(c) : x^M calculated from Motomura , Scamehorn , Yu and Rubingh's methods for Cu / $C_{12}E_8$ system

α	x^M (Motomura)	x^M (Scamehorn)	x^M (Yu)	x^M (Rubingh)
0.50	0.34	0.33	0.42	0.35
0.70	0.53	0.52	0.46	0.54
0.80	0.65	0.65	0.49	0.68

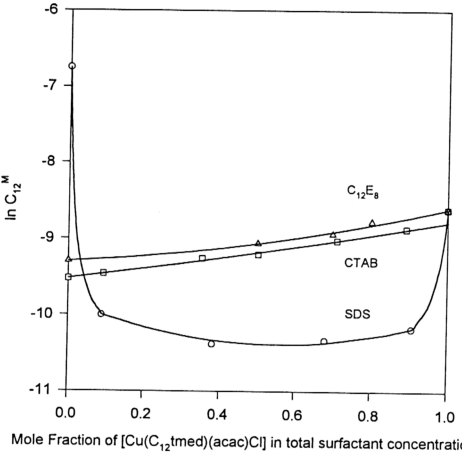

Figure 3-17 : Plot of ln $\ln C_{12}^{M}$ versus α for Cu / SDS , Cu / CTAB and Cu / $C_{12}E_8$ systems

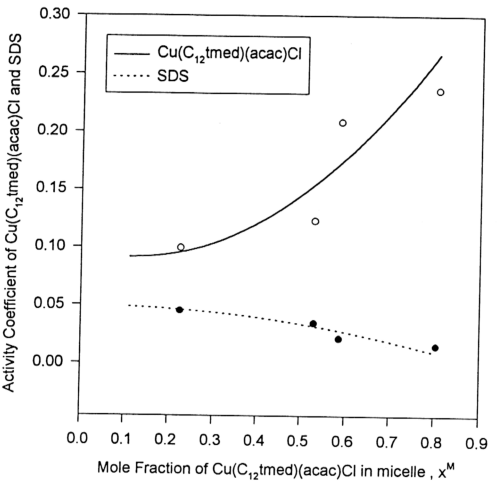

Figure 3-18 : Plot of f_1^M and f_2^M versus x^M for Cu / SDS systems based on Scamehorn's method

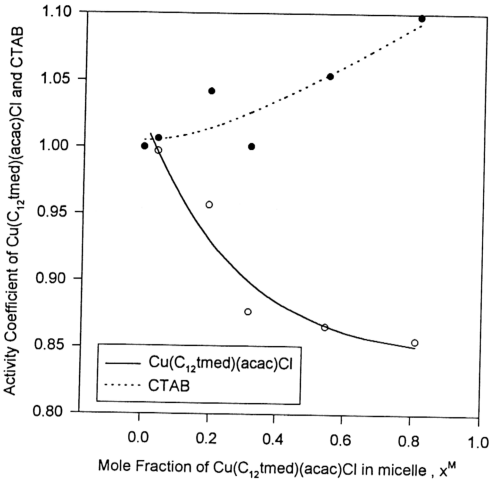

Figure 3-19 : Plot of f_1^M and f_2^M versus x^M for Cu / CTAB systems based on Scamehorn's method

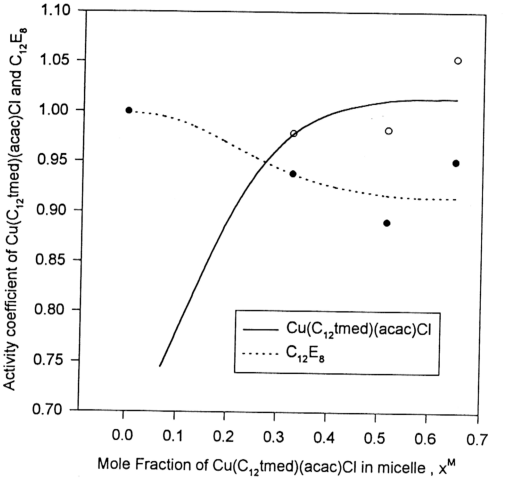

Figure 3-20 : Plot of f_1^M and f_2^M versus x^M for Cu / $C_{12}E_8$ systems based on Scamehorn's method

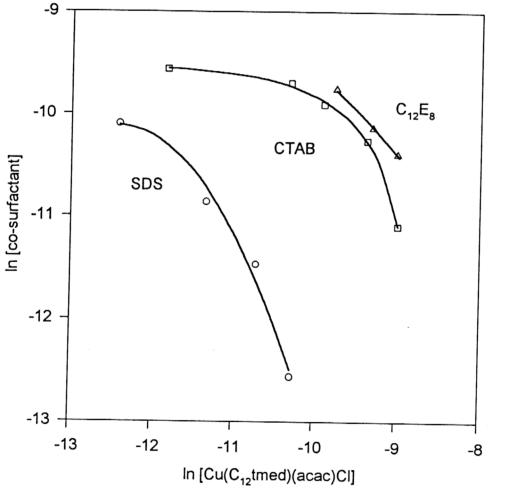

Figure 3-21 : $\ln C_{2m}$ versus $\ln C_{1m}$ for Cu / SDS and Cu / CTAB and Cu / $C_{12}E_8$ systems

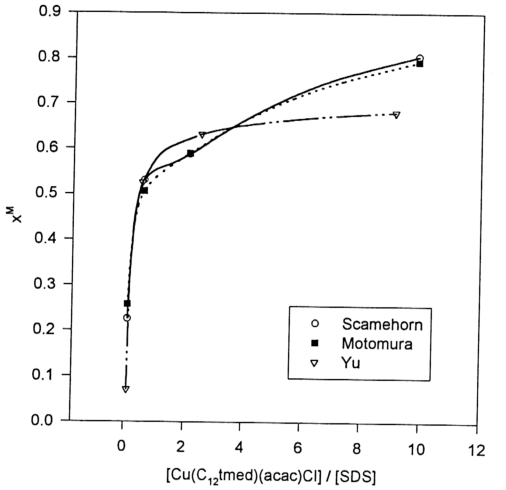

Figure 3-22 : Plots of x^M versus [Cu] / [SDS] calculated from Scamehorn , Yu and Motomura's methods

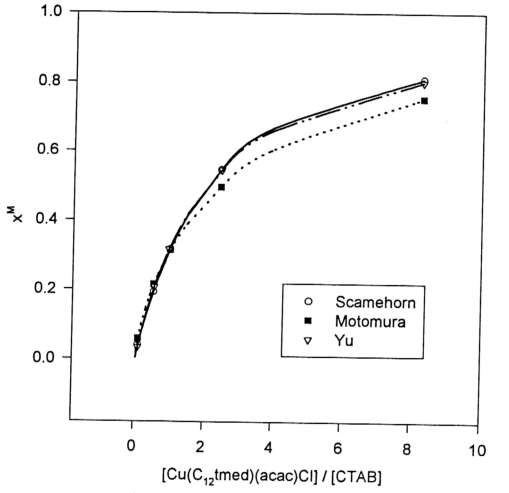

Figure 3-23 : Plots of x^M versus [Cu] / [CTAB] calculated from Scamehorn , Yu and Motomura's methods

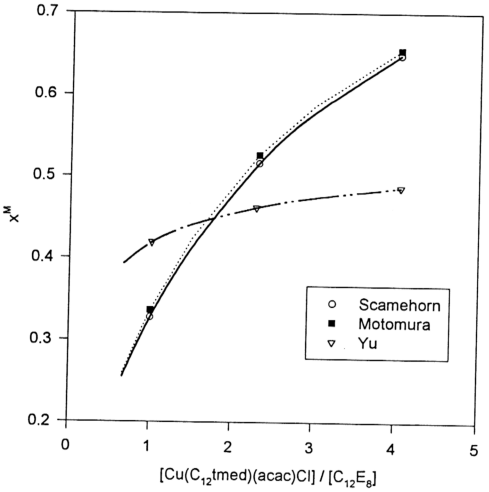

Figure 3-24 : Plots of x^M versus [Cu] / [$C_{12}E_8$] calculated from Scamehorn , Yu and Motomura's methods

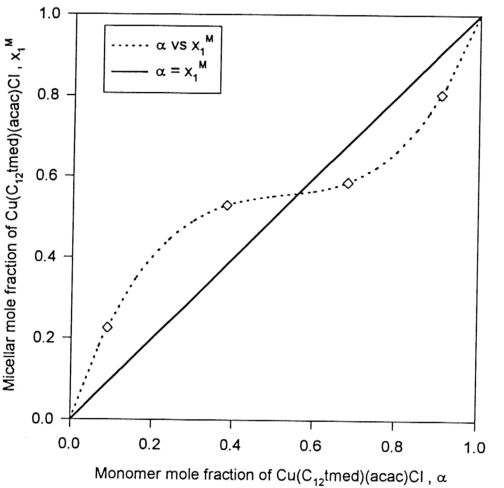

Figure 3-25 : Variation of the micellar phase composition with monomer phase composition for Cu / SDS mixtures based on Scamehorn's method

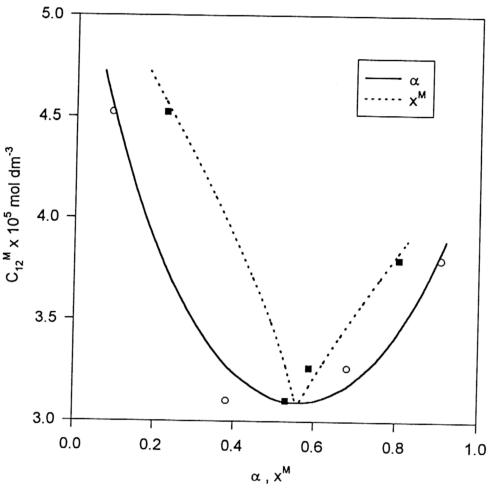

Figure 3-26 : Variation of the mixture CMC C_{12}^{M} with monomer α and micellar phase composition x^{M} for mixtures of Cu / SDS system calculated from the Scamehorn's method

(III) Other methods of estimating micellar interaction - effects of counterion dissociation

Some authors derived equation by taking into account the counterion binding constant , especially in systems involving fluorocarbon-hydrocarbon mixed surfactants [27,31,32,42,96] . Counterion binding constants K_g calculated using Evan's method (based on conductivity data) for surfactants $Cu(C_{12}tmed)(acac)Cl$, SDS and CTAB are tabulated in Table 3-22 .

Table 3-22 : Micellar ionization degrees and counterion binding constants obtained based on Evan's equation

Compound	Micellar Ionization Degree	Counterion binding constant K_g
$Cu(C_{12}tmed)(acac)Cl$	0.29 [11(d)]	0.71
SDS	0.256 [97]	0.744
CTAB	0.22 [98]	0.78
$C_{12}E_8$	0	0

Rubingh's equation had been expanded to include additional interaction parameter δ by Fung et. al. [31].

$$\frac{1}{\left(1-\left(x^M\right)^2\right)}\ln\left[\frac{\left(\alpha C_{12}^M\right)^{1+K_{g1}}}{x^M\left(C_1^M\right)^{1+K_{g1}}}\right]=\frac{1}{\left(x^M\right)^2}\ln\left[\frac{\left((1-\alpha)C_{12}^M\right)^{1+K_{g2}}}{\left(1-x^M\right)\left(C_2^M\right)^{1+K_{g2}}}\right]-\frac{\delta}{2} \qquad (3\text{-}42)$$

$$\beta^M=\frac{1}{\left(1-\left(x^M\right)^2\right)}\ln\left[\frac{\left(\alpha C_{12}^M\right)^{1+K_{g1}}}{x^M\left(C_1^M\right)^{1+K_{g1}}}\right]-\delta(1-x)+\frac{\delta}{2}=\frac{1}{\left(x^M\right)^2}\ln\left[\frac{\left((1-\alpha)C_{12}^M\right)^{1+K_{g2}}}{\left(1-x^M\right)\left(C_2^M\right)^{1+K_{g2}}}\right]-\delta(1-x) \qquad (3\text{-}43)$$

where K_{g1} , K_{g2} = degrees of counterion binding of surfactants 1 , 2

In the mixed surfactant system , at least two factors are involved in the process : (I) head group interaction , which is characterized by β^M (II) carbon chain (hydrocarbon and fluorocarbon) compatibility , which can be characterized by δ . The former is related to electrostatic interaction between the head groups , while the latter is responsible for the hydrophobic interaction between the chains . Compatible chains result in maximum cohesive interactions between the alkyl groups while incompatible chains have a disruptive effect on the packing of molecules in the micelles [99] . The δ value can be related to the difference in the partial molar volumes of the pure component and the mixed systems [31] . Positive deviations of δ indicate an increase in the area / volume ($\Delta V > 0$) occupied by either one or both components , probably due to a more repulsive interaction in nature , whereas negative deviations are indicative of condensation ($\Delta V < 0$) [100] . The most pronounced condensing effect is usually observed when the two components have equal chain length . [99] .

For each α only one parameter (β^M or δ) can be calculated . Hence the calculated value of β^M depends on δ . The pair of β^M and δ values which best fit the experimental data set (C_{12}^M versus α) is determined from minimization of least squares function F (see appendix for detail)

$$F = \sum_{i=1}^{N} \left[\left(C_{12}^{M,\text{expt}} \right)_i - \left(C_{12}^{M,\text{calc}} \right)_i \right]^2 \qquad (3\text{-}44)$$

Table 3-23 : Micellar interaction parameters β^M and δ based on Fung's equation

System	Fung		Rubingh
	β^M	δ	β^M
Cu - SDS	-21.35	0.6	-10.9
Cu - CTAB	-2.38	-1.1	-0.12
Cu - $C_{12}E_8$	-1.57	2.0	-0.13

The calculated micellar interaction parameter β^M and mole fraction x^M values are tabulated in Table 3-23 . When compared with β^M calculated from Rubingh's equation , Fung's method always gives higher magnitude of β^M values . The increase in magnitude is almost twice in Cu / SDS system , -10.9 (Rubingh) versus -21.35 (Fung) . In Cu / CTAB and Cu / $C_{12}E_8$, higher values are also obtained , -2.38 and -1.57 from Fung's method , as compared to -0.12 and -0.13 from Rubingh's equation . The negative β^M values reflect that there are attractive interaction between the two type of surfactant head group upon micellization . δ values are small compared to those of the hydrocarbon / fluorocarbon systems , where values of 6 an 14.7 have been reported [31] . Small to moderate positive δ values are obtained in Cu / SDS and Cu / $C_{12}E_8$ systems , which correspond to small mutual phobicity between the hydrocarbon / hydrocarbon chains , while negative δ value in Cu / CTAB system (with different chain length) exhibits good miscibility behavior in the hydrocarbon / hydrocarbon chain . However the effect of β^M is more important than δ so that the overall interaction free energy is more favorable for the formation of mixed micelles . The plots of C_{12}^M versus α for three systems fit well with those predicted from Fung's model as shown in Figures 3-27 , 3-28 and 3-29 .

Rubingh's equation had also been modified by Esumi et. al. [32] where the counterion effect and binding in binary mixtures is considered

$$\beta^M = \frac{\ln\left[\dfrac{\alpha\left(C_{12}^M\right)^{1+K_g}}{x^M\left(C_1^M\right)^{1+K_{g1}}}\right]}{\left(1-x^M\right)^2} = \frac{\ln\left[\dfrac{(1-\alpha)\left(C_{12}^M\right)^{1+K_g}}{\left(1-x^M\right)\left(C_2^M\right)^{1+K_{g2}}}\right]}{\left(x^M\right)^2} \qquad (3\text{-}45)$$

$$K_g = x^M K_{g1} + (1-x^M)K_{g2} \qquad (3\text{-}46)$$

where

K_g = degree of counterion binding of the mixtures

β^M and x^M for binary surfactant mixtures of Cu / SDS , Cu / CTAB and Cu / $C_{12}E_8$ are calculated and tabulated in Table 3-24(a) to 3-24(c) . Esumi's method also gives higher β^M values when compared to Rubingh's equation . For some mixtures of Cu / CTAB and Cu / $C_{12}E_8$ systems , Esumi's method is unable to obtain any results as there is no solution to the equation for x^M .

Kamrath and Franses find out that for ionic surfactants , β^M and x^M are substantially sensitive to the value of K_g [27(a)] . This sensitivity indicates that the nonionic micellization model (i.e. K_g = 0 , Rubingh's equation) is inadequate for describing the micellar mixing of ionic surfactants . **However , in swamping electrolytes , mixed CMC's of ionic surfactants can be calculated via the nonionic surfactant model [27(a)] , as what had been done in the early part of this thesis .**

Table 3-24(a) : Micellar interaction parameter and mole fraction of $Cu(C_{12}tmed)(acac)Cl$ in Cu / SDS system based on Esumi's equation

α	β^M	x^M
0.09	-18.3	0.52
0.38	-18.4	0.56
0.68	-17.8	0.59
0.91	-17.9	0.63
Average	-18.1 ± 0.3	-

Table 3-24(b) : Micellar interaction parameter and mole fraction of $Cu(C_{12}tmed)(acac)Cl$ in Cu / CTAB system based on Esumi's equation

α	β^M	x^M
0.09	-	-
0.35	-	-
0.50	0.28	0.08
0.71	0.10	0.20
0.89	-0.48	0.48
Average	-0.03 ± 0.3	-

Table 3-24(c) : Micellar interaction parameter and mole fraction of $Cu(C_{12}tmed)(acac)Cl$ in Cu / $C_{12}E_8$ system based on Esumi's equation

α	β^M	x^M
0.50	-5.9	0.83
0.70	-5.5	0.89
0.80	-	-
Average	-5.7 ± 0.2	-

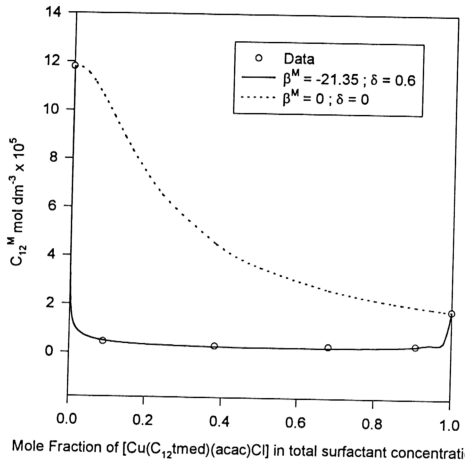

Figure 3-27 : C_{12}^{M} versus α for binary mixtures of Cu / SDS system calculated with Fung's equation .

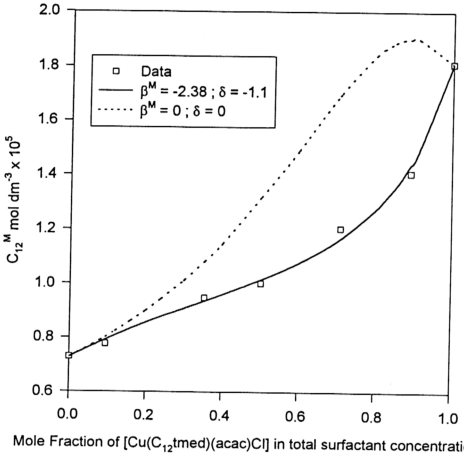

Figure 3-28 : C_{12}^{M} versus α for binary mixtures of Cu / CTAB system calculated with Fung's equation .

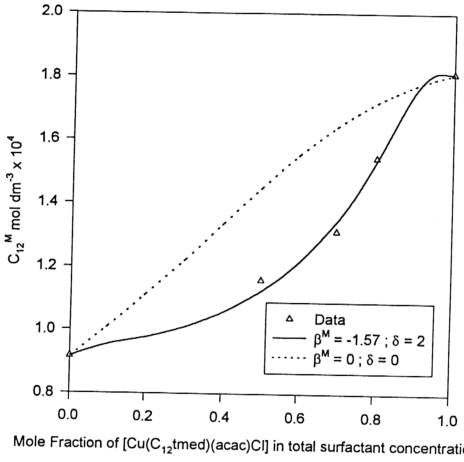

Figure 3-29 : C_{12}^{M} versus α for binary mixtures of Cu / $C_{12}E_8$ system calculated with Fung's equation .

(B) UV-Visible Studies

As can be seen from Figures 3-31 to 3-35 , a single broad adsorption band is observed around 600 nm . This broad band is a composite band with the contribution from the following three transitions :

$$d_{z^2} \rightarrow d_{x^2-y^2} \; ; \; d_{xy} \rightarrow d_{x^2-y^2} \text{ and } d_{xz}, d_{yz} \rightarrow d_{x^2-y^2}$$

As the axial interaction increases (Figure 3-30) , the three absorption energies decrease because of the decreased tetragonal distortion . Hence wavenumber $\bar{\nu}$ (in cm^{-1}) will decrease as axial interaction increases [90] . UV spectra had been used to study the arrangement of Cu(II) head groups in micelles [11(a)] . It is found that as micellization is enhanced , $\bar{\nu}_{max}$ (wavenumber , cm^{-1}) is decreased i.e. λ_{max} (wavelength, nm) is increased . The molar absorptivity (ε) also tends to increase with increasing micellization .

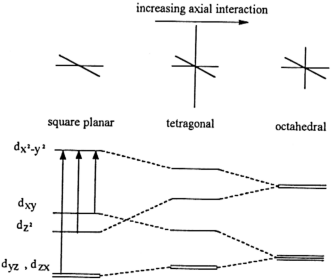

Figure 3-30 : An energy level diagram showing the effect of increasing interaction at the axial position of a square planar complex .

The change of $\bar{\nu}_{max}$ with concentration of the Cu(II) surfactant and with addition of NaCl suggest an octahedral structure for the Cu(II) complex in the micellar head groups . The structure of square planar and octahedral complex are shown below .

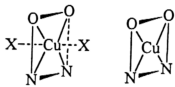

Octahedral Square Planar

UV-Visible spectra of [Cu(C_{12}tmed)(acac)Cl] / SDS mixtures in water and the resultant $\bar{\nu}_{max}$ and ε_{max} values are shown in Figure 3-31 and Table 3-25 respectively . It is found that adding SDS into Cu(C_{12}tmed)(acac)Cl only slightly increases $\bar{\nu}_{max}$ and ε_{max} values .

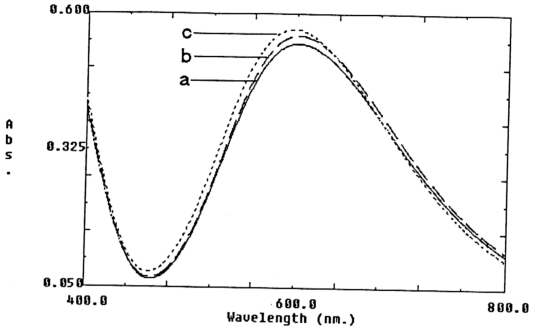

Figure 3-31 : UV-Visible spectra of [Cu(C_{12}tmed)(acac)Cl] / SDS mixtures in water .

Table 3-25 : $\bar{\nu}_{max}$ and ε_{max} values of [Cu(C_{12}tmed)(acac)Cl] / SDS mixtures in water .

No.	[Cu(C_{12}tmed)(acac)Cl] mM	[SDS] mM	α_{Cu}	$\bar{\nu}_{max}$ (10^3 cm^{-1})	ε_{max} (M^{-1} cm^{-1})
a	5	0	1	16.68	108
b	5	1.5	0.8	16.68	111
c	5	20	0.23	16.81	114

α_{Cu} = mole ratio of Cu(C_{12}tmed)(acac)Cl in mixed Cu(C_{12}tmed)(acac)Cl/SDS system .

UV-Visible spectra of [Cu(C_{12}tmed)(acac)Cl] / SDS mixtures in 0.1 M NaCl and the resultant $\bar{\nu}_{max}$ and ε_{max} values are shown in Figure 3-32 and Table 3-26 respectively . Same trend is observed as in water solution . When SDS is added to Cu(C_{12}tmed)(acac)Cl , the CMC of the mixture is very much lower than the individual surfactant . Micellization process is enhanced . The increase in wavenumber is consistent with the appearance of a high field ESR peak in the presence of higher concentration of SDS , which is interpreted as due to the increase in the Cu--Cu head group distance resulting from the displacement of chloride by the sulfate group . (see discussion in Chapter 3 (C)(iv))

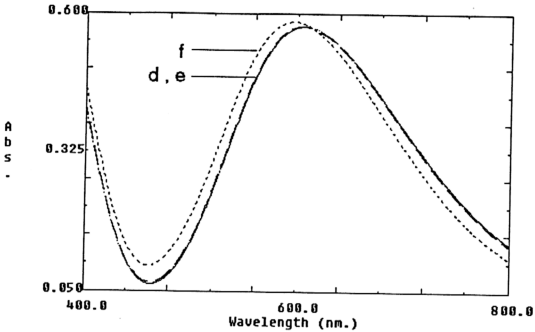

Figure 3-32 : UV-Visible spectra of [Cu(C_{12}tmed)(acac)Cl] / SDS mixtures in 0.1 M NaCl .

Table 3-26 : $\bar{\nu}_{max}$ and ε_{max} values of Cu(C_{12}tmed)(acac)Cl / SDS mixtures in 0.1 M NaCl .

No.	[Cu(C_{12}tmed)(acac)Cl] (mM)	[SDS] (mM)	α_{Cu}	$\bar{\nu}_{max}$ (10^3 cm^{-1})	ε_{max} (M^{-1} cm^{-1})
d	5	0	1	16.52	115
e	5	1.5	0.8	16.52	115
f	5	20	0.23	16.78	117

α_{Cu} = mole ratio of Cu(C_{12}tmed)(acac)Cl in mixed Cu(C_{12}tmed)(acac)Cl/SDS system .

UV-Visible spectra of [Cu(C_{12}tmed)(acac)Cl] / CTAB mixtures in 0.1 M NaCl and the resultant $\bar{\nu}_{max}$ and ε_{max} values are shown in Figure 3-33 and Table 3-27 respectively . The result shows that adding CTAB into Cu(C_{12}tmed)(acac)Cl slightly increases ε_{max} and slightly decreases the wavenumber . The decrease in wavenumber and increase in absorbance of the absorption band , indicate that adding CTAB into copper surfactant enhances the micellization . Similar to the Cu(C_{12}tmed)(acac)Cl / SDS system , in the ESR spectrum (Figure 3-42) , the high field peak is more evident for the mixed micelle as compared to pure copper micelle , indicating that the Cu--Cu head group distance is lengthened . This seems to suggest that Cu...N^+...Cu and Cu...Cl^-...Cu may contribute to the micellar head group more than that from Cu...Br^- ...Cu . Note that Cu...N^+...Cu arrangement would increase $\bar{\nu}_{max}$ but Cu...Cl^-...Cu would decrease $\bar{\nu}_{max}$. The opposing effects of these two structures would therefore cause a small change in $\bar{\nu}_{max}$. (Note : ligand field strength of Cl is stronger than Br) .

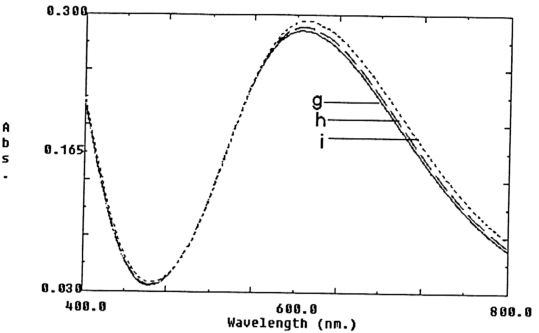

Figure 3-33 : UV-Visible spectra of [Cu(C_{12}tmed)(acac)Cl] / CTAB mixtures in 0.1 M NaCl .

Table 3-27 : $\bar{\nu}_{max}$ and ε_{max} values of [Cu(C_{12}tmed)(acac)Cl] / CTAB mixtures in 0.1 M NaCl .

No.	[Cu(C_{12}tmed)(acac)Cl] mM	[CTAB] mM	α_{Cu}	$\bar{\nu}_{max}$ (10^3 cm^{-1})	ε_{max} (M^{-1} cm^{-1})
g	2.5	0	1	16.49	114
h	2.5	0.625	0.8	16.49	115
i	2.5	10	0.2	16.39	118

α_{Cu} = mole ratio of Cu(C_{12}tmed)(acac)Cl in mixed Cu(C_{12}tmed)(acac)Cl/CTAB system .

UV-Visible spectra of [Cu(C_{12}tmed)(acac)Cl] / $C_{12}E_8$ mixtures in water and the resultant $\bar{\nu}_{max}$ and ε_{max} values are shown in Figure 3-34 and Table 3-28 respectively . Adding $C_{12}E_8$ into Cu(C_{12}tmed)(acac)Cl slightly decreases the wavenumber and increases the absorbance . Here , the increase of micellization would decrease the wavenumber and increase absorbance , but the plausible displacement of Cl^- ion by the oxyethylene group would increase or decrease $\bar{\nu}_{max}$ depending on its strength of interaction with the copper center relative to that of chloride . As we do not have information on this , the only small change in $\bar{\nu}_{max}$ may mean that this effect (from oxyethylene) is small .

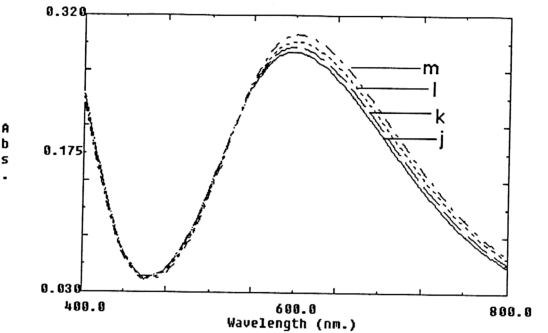

Figure 3-34 : UV-Visible spectra of [Cu(C_{12}tmed)(acac)Cl] / $C_{12}E_8$ mixtures in water .

Table 3-28 : $\bar{\nu}_{max}$ and ε_{max} values of [Cu(C_{12}tmed)(acac)Cl] / $C_{12}E_8$ mixtures in water .

No.	[Cu(C_{12}tmed)(acac)Cl] (mM)	[$C_{12}E_8$] (mM)	α_{Cu}	$\bar{\nu}_{max}$ (10^3 cm^{-1})	ε_{max} (M^{-1} cm^{-1})
j	2.45	0	1	16.75	115
k	2.45	0.631	0.8	16.67	117
l	2.45	2.47	0.5	16.64	120
m	2.45	10.02	0.2	16.64	122

α_{Cu} = mole ratio of Cu(C_{12}tmed)(acac)Cl in mixed Cu(C_{12}tmed)(acac)Cl/$C_{12}E_8$ system .

UV-Visible spectra of [Cu(C_{12}tmed)(acac)Cl] / $C_{12}E_8$ mixtures in 0.1 M NaCl and the resultant $\bar{\nu}_{max}$ and ε_{max} values are shown in Figure 3-35 and Table 3-29 respectively . Although it appears that adding $C_{12}E_8$ into Cu(C_{12}tmed)(acac)Cl slightly increases the wavenumber and increases the absorbance , the change however is too small for us to offer any meaningful interpretation .

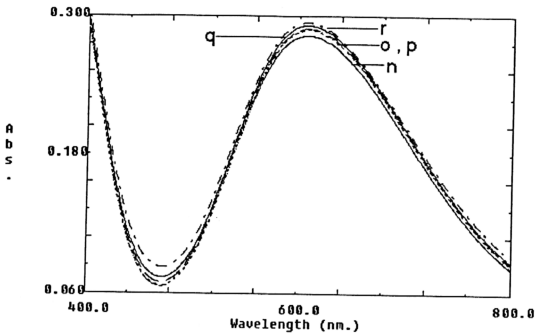

Figure 3-35 : UV-Visible spectra of [Cu(C_{12}tmed)(acac)Cl] / $C_{12}E_8$ mixtures in 0.1 M NaCl .

Table 3-29 : $\bar{\nu}_{max}$ and ε_{max} values of [Cu(C_{12}tmed)(acac)Cl] / $C_{12}E_8$ mixtures in 0.1 M NaCl .

No.	[Cu(C_{12}tmed)(acac)Cl] (mM)	[$C_{12}E_8$] (mM)	α_{Cu}	$\bar{\nu}_{max}$ (10^3 cm^{-1})	ε_{max} (M^{-1} cm^{-1})
n	2.58	0	1	16.41	110
o	2.58	0.655	0.8	16.41	112
p	2.58	2.57	0.5	16.41	112
q	2.58	5.0	0.34	16.49	113
r	2.58	10.0	0.2	16.50	114

α_{Cu} = mole ratio of Cu(C_{12}tmed)(acac)Cl in mixed Cu(C_{12}tmed)(acac)Cl/$C_{12}E_8$ system .

(C) Electron Spin Resonance (ESR) Studies

Typically a monomeric Cu^{2+} ($I=\frac{3}{2}$ for ^{63}Cu (69.1%) and ^{65}Cu (30.9%)) complex shows a 4-line (2I+1) spectrum in solution due to coupling to the nuclear spin and the nearly equal magnetogyric ratio of ^{63}Cu and ^{65}Cu . The $m_I = \frac{3}{2}$ component has the highest intensity .

(i) ESR Studies of $Cu(CH_3\text{-tmed})(acac)Cl$ in 0.1 M NaCl

$Cu(CH_3\text{-tmed})(acac)Cl$ is a non-surface active copper complex . Both $Cu(CH_3\text{-tmed})(acac)Cl$ in water and 0.1 M NaCl give very well resolved 4-line spectrum , (g_{iso} = 2.114 ; A_{iso} = 80.1 G) . In the presence of 20 mM SDS , however , the 3 low-field peaks are less resolved (Figure 3-36 , Plot 2). The partially resolved spectrum is probably due to the restricted motion of the copper cation in the Stern layer of SDS micelle .

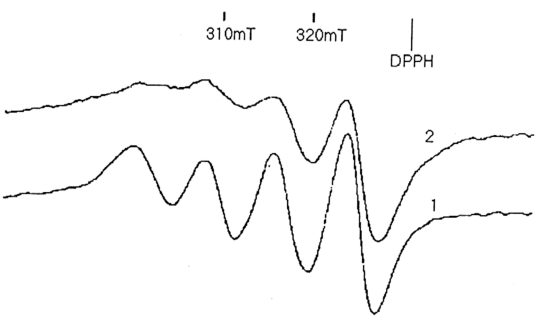

Figure 3-36 : ESR spectra for 5 mM [$Cu(CH_3\text{-tmed})(acac)Cl$] in 0.1 M NaCl :

(1) without SDS , (2) with 20 mM SDS

(ii) ESR Studies for [Cu(C_{12}tmed)(acac)Cl] in water

It has been reported that the ESR spectra of [Cu(C_{12}tmed)(acac)Cl] in water are very sensitive to concentration changes [11(a)] . When the concentrations are lower than CMC , a typical well resolved four-line spectrum was obtained (Figure 3-37) . As the concentration increases , the signal corresponding to the $+\frac{1}{2}$ component becomes broader , and more intense , while $+\frac{3}{2}$ component become relatively less intense , and finally a broad signal centered at ~ 317 mT was obtained . This broad band is caused by formation of micelles in the solution . The line-broadening has been attributed mainly to the electron spin - electron spin dipolar interaction . An increase of line width indicates a decrease in the inter head group distance [11(a)] .

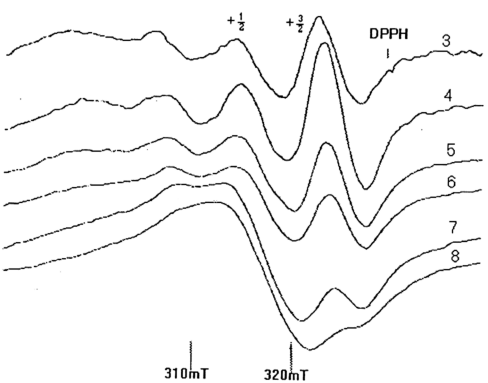

Figure 3-37 : ESR spectra of [Cu(C_{12}tmed)(acac)Cl] in water at the various concentrations : (3) 0.29 , (4) 1.09 , (5) 2.28 , (6) 3.18 , (7) 6.32 , (8) 12.93 mM

(iii) ESR Studies for [Cu(C_{12}tmed)(acac)Cl] / SDS mixtures in water

A 5 mM of [Cu(C_{12}tmed)(acac)Cl] solution (Figure 3-38) exhibits a spectrum that lies between plot 6 (3.18 mM) and plot 7 (6.32 mM) in Figure 3-37 . The spectrum observed is a composite spectrum , which is the sum of micelle and monomer peaks . When little SDS (1.5 mM) is added , the spectrum is almost unchanged (Figure 3-38 ,plot 10) . In the presence of excess SDS (20 mM) (Figure 3-38 , plot 11) , the ESR spectrum becomes less resolved because of the expected lower CMC values and there is an additional high field peak at ~326 mT . The micellar peak is obtained at ~317 mT .

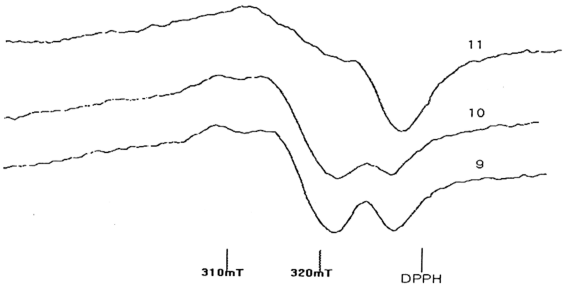

Figure 3-38 : ESR spectra of 5 mM [Cu(C_{12}tmed)(acac)Cl] in water :

(9) without SDS , (10) 1.5 mM SDS , (11) 20 mM SDS

(iv) ESR Studies for [Cu(C_{12}tmed)(acac)Cl] / SDS mixtures in 0.1 M NaCl

In Figure 3-39 , the ESR spectrum of pure copper surfactant complex in 0.1 M NaCl gives a broad micellar peak , indicating enhanced micellization in the saline solution . The monomer peak is not detectable because of the extremely low CMC value (1.8×10^{-4} M) . As SDS is added , the high-field peak becomes more conspicuous and with excess of SDS (20 mM) added (Figures 3-40 and 3-41), a well resolved high field peak is obtained . We believe that this peak is part of the spectrum arising from the bridged Cu....O-S-O....Cu head group of which the Cu.....Cu distance is much longer than that of the Cu....Cl....Cl head group ; the latter gives rise to the broad signal (centered at ~317 mT) . The DS-separated copper gives a monomer-like spectrum because of the increased Cu....Cu distance .

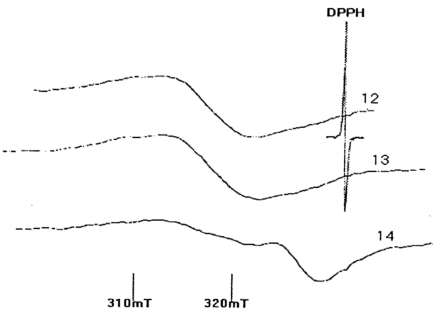

Figure 3-39 : ESR spectra of 5 mM [Cu(C_{12}tmed)(acac)Cl] in 0.1 M NaCl :

(12) without SDS , (13) 1.5 mM SDS , (14) 20 mM SDS

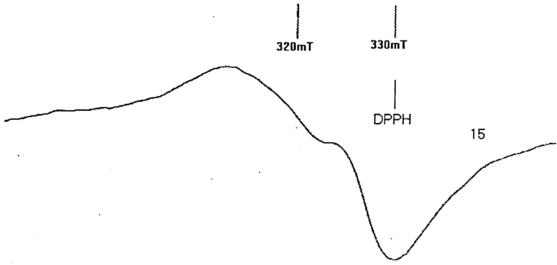

Figure 3-40 : ESR spectra of 5 mM [Cu(C_{12}tmed)(acac)Cl] and 20 mM SDS in 0.1 M NaCl (15)

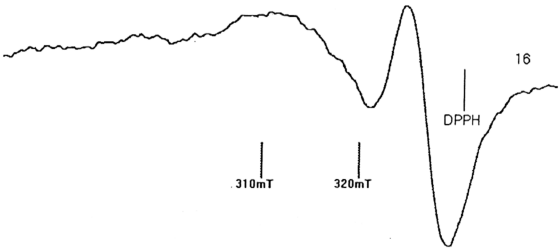

Figure 3-41 : ESR spectra of 2.5 mM [Cu(C_{12}tmed)(acac)Cl] and 20 mM SDS in 0.1 M NaCl (16)

(v) ESR Studies for [Cu(C_{12}tmed)(acac)Cl] / CTAB mixtures in 0.1 M NaCl

When small amount of CTAB (0.66 mM) is added the spectrum does not change much (Figure 3-42 , plots 17 and 18) . But when excess CTAB (10 mM) is added , a well resolved high field peak is obtained similar to that of SDS as co-surfactant (Figure 3-42 , plot 19) . Here again the copper is in two types of environment , *viz.* , Cu...X....Cu (X = Cl , Br) and Cu....NR($Me)_3$....Cu where the former gives rise to the broad signal at ~317 mT and the latter gives rise to the sharp signal at ~326 mT .

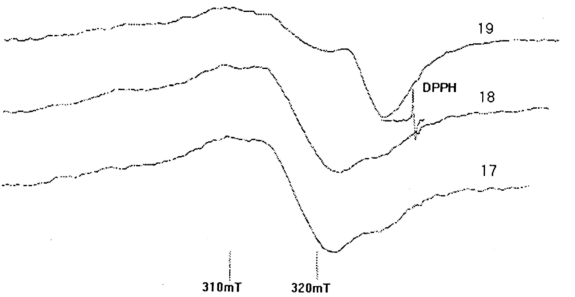

Figure 3-42 : ESR spectra of 2.53 mM [Cu(C_{12}tmed)(acac)Cl] in 0.1 M NaCl :

(17) without CTAB , (18) 0.66 mM CTAB , (19) 10 mM CTAB

(vi) ESR Studies of [Cu(C_{12}tmed)(acac)Cl] / $C_{12}E_8$ mixtures in water and 0.1 M NaCl

Similar to the case of [Cu(C_{12}tmed)(acac)Cl] / SDS in water , the introduction of $C_{12}E_8$ will enhance micellization of copper surfactant . The addition of $C_{12}E_8$ reduces CMC of copper surfactant , i.e. $C_{12}E_8$ increases micellar and decreases monomer content . Therefore adding equimolar of $C_{12}E_8$ (5 mM) to copper surfactant , will produce micellar peak , similar to pure copper surfactant in plot 8 (12.63 mM) in Figure 3-37 [11(a)] .

In 0.1 M NaCl , with excess of $C_{12}E_8$, a well resolved of high field peak is also observed (Figure 3-44 , plot 25) similar to SDS (Figure 3-40) and CTAB (Figure 3-42 , plot 19) , suggesting that $C_{12}E_8$ is also inserted between the two copper(II) head groups in the mixed micelle .

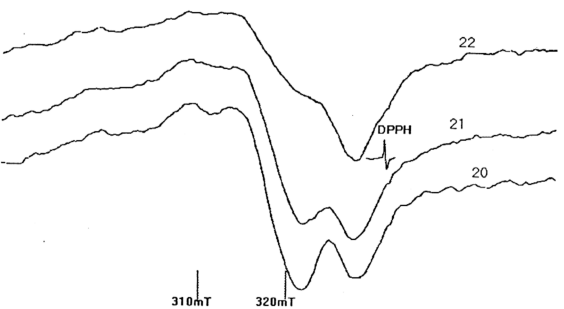

Figure 3-43 : ESR spectra of 5.2 mM [Cu(C_{12}tmed)(acac)Cl] in water :

(20) without $C_{12}E_8$, (21) 1.31 mM $C_{12}E_8$, (22) 5.2 mM $C_{12}E_8$

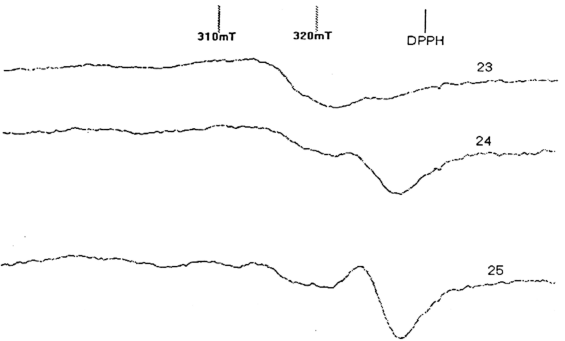

Figure 3-44 : ESR spectra of 2.58 mM [Cu(C_{12}tmed)(acac)Cl] in 0.1 M NaCl :

(23) without $C_{12}E_8$, (24) 5 mM $C_{12}E_8$, (25) 10 mM $C_{12}E_8$

Conclusion :

(1) For copper surfactant in water , with addition of SDS and $C_{12}E_8$, the diminishing monomer signal is due to decrease of CMC , with formation of mixed micelle .

(2) For copper surfactant in 0.1 M NaCl ,with addition of SDS , CTAB and $C_{12}E_8$, the presence of the high field peak is not due to monomeric copper surfactant (CMC is very much reduced) , but due to the presence of mixed head group arrangements such as (I) or (II) in Figure 3-55 , shown below :

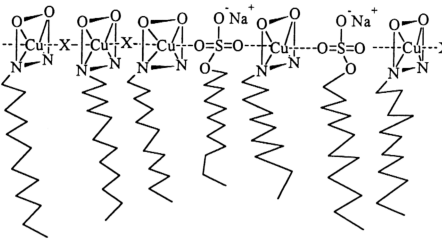

Figure 3-55 (I) : A proposed arrangement of the head groups with sulfate head group $-O-SO_3^-$ from *SDS* displacing some Cl^- anion in the mixed micelle .

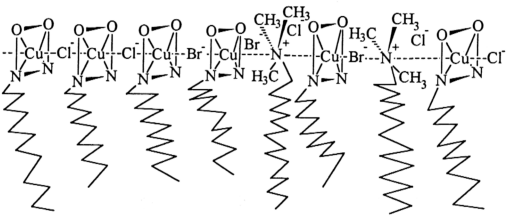

Figure 3-55 (II) : A proposed arrangement of the head groups with nonbonded alkyl ammonium head group displacing some Cl^- in the mixed micelle .

Note that in the same way , the hydrophilic head group of $C_{12}E_8$ takes the place of sulphate or alkyl ammonium head group in the Cu / $C_{12}E_8$ mixed micelle .

(D) Kinetic Studies of Mixed Micelles System

(I) Autooxidation of 3,5-di-*tert*-butylcatechol (3,5-DTBC)

Effects of co-surfactants , SDS (anionic) , CTAB (cationic) and $C_{12}E_8$ (nonionic) , on the rate of autooxidation of 3,5-di-*tert*-butylcatechol (3,5-DTBC) at pH 5.7 in the presence of copper micellar solution (i.e. $Cu(C_{12}tmed)(acac)Cl$, $Cu(C_{16}tmed)(acac)Cl$, $Cu(C_{12}tmed)Br_2$) had been investigated . The effects of co-surfactant were studied by varying concentration of co-surfactant while fixing copper concentration at 0.5 or 1 mM . The CMC values of the pure surfactants in water are listed in Table 3-30 . Since the concentrations of Cu(II) surfactants studied are near or above the CMC values , the reaction can be considered in term of micellar effects instead of monomer effects . Addition of cosurfactant into copper surfactant solutions will immediately form mixed micellar solutions .

Table 3-30 : CMC values of the pure surfactants in water

Compound	CMC / 10^{-3} M
SDS	8.0
CTAB	0.92
$C_{12}E_8$	0.86
$Cu(C_{12}tmed)(acac)Cl$	0.92
$Cu(C_{16}tmed)(acac)Cl$	0.04
$Cu(C_{12}tmed)Br_2$	0.97

Due to low solubility of 3,5-DTBC in water (solubility $\leq$ (2-3) x 10^{-4} M) , the substrate was prepared in acetonitrile . The reaction was carried out under the condition of excess surfactants over substrate and monitored at 385 nm . The UV spectra of

autooxidation of 3,5-DTBC in different co-surfactant media are shown in Figures 3-46 , 3-47 and 3-48 . The oxidized product is indicated by the appearance of the absorption maximum at 385 nm . This value is close to the range of 390-420 nm reported in literature for 3,5-di-*tert*-butyl-*o*-benzoquinone (3,5-DTBQ) (ε_{404nm} = 1.58 x 10^3 M^{-1} cm^{-1} ; 0.1 M KNO_3 , 50% methanol) [102] .

Typical time course spectra are shown in Figure 3-49 . Some more time course spectra are listed in appendix V for further reference . In the analysis of the time-dependence absorption data , first order kinetics with respect to 3,5-DTBC is assumed . The observed rate constants is calculated according to following equation :

$$A_{obs} - A_{Cu} = \varepsilon_q C_0 - \varepsilon_q C_0 e^{-k_{obs} l} e^{-k_{obs} t} \qquad (3\text{-}47)$$

where

A_{obs} = observed absorbance

A_{Cu} = absorbance of the Cu(II) complex in the presence of co-surfactant

ε_q = molar absorptivity of 3,5-DTBQ

C_0 = concentration of 3,5-DTBQ formed

k_{obs} = observed rate constant

l = the time interval between mixing the reactants and the starting of the measurement at an appropriate wavelength

t = time when a reading is taken

Equation above can be simplified as below

$$Y = A(1) - A(2)\exp[-A(3) * X] \qquad (3\text{-}48)$$

where

$Y = A_{obs} - A_{Cu}$

$X = t$

$A(1) = \varepsilon_q C_0$

$A(2) = \varepsilon_q C_0 e^{-k_{obs}t}$

$A(3) = k_{obs}$

$A(1)$, $A(2)$, $A(3)$ are the parameters to be determined . The observed first order rate constants (k_{obs}) were obtained by fitting experimental curves to the first order rate equation using Peakfit program developed by Jandel Scientific .

The calculated k_{obs} values for the pure surfactants alone are tabulated in Table 3-31 .

Table 3-31 : The values of k_{obs} for the autooxidation of 3,5-DTBC in the micellar solutions at 25°C and pH = 5.7

Compound	Concentration 10^3 M	k_{obs} 10^4 s^{-1}
SDS	1.0	1.2
CTAB	1.0	8
$C_{12}E_8$	3.8	0.015
$Cu(C_{12}tmed)(acac)Cl$	1.0	112
$Cu(C_{16}tmed)(acac)Cl$	0.5	17
$Cu(C_{12}tmed)Br_2$	0.5	119

The autooxidation rate of 3,5-DTBC in the presence of SDS , CTAB or $C_{12}E_8$ alone is extremely slow .

The effects of increasing concentration of the co-surfactants on the observed rate constants are plotted in Figures 3-50, 3-51 and 3-52 . SDS is not included in Figure 3-52 due to turbidity formation when the ratio of concentration of SDS to $[Cu(C_{12}tmed)Br_2]$ is less than 4 . The three surface active copper(II) surfactants exhibit different rate effects on mixing with the co-surfactant . In all the mixed surfactant systems involving

[$Cu(C_{16}tmed)(acac)Cl$] , the rate increases on increasing the co-surfactant concentration . In the [$Cu(C_{12}tmed)(acac)Cl$] system , the rate decreases when the co-surfactant is SDS and CTAB , but increases when it is $C_{12}E_8$. In the [$Cu(C_{12}tmed)Br_2$] system , the rate increases when the co-surfactant is CTAB and $C_{12}E_8$. When SDS is added as the co-surfactant the rate decreases from 0.039 s^{-1} in 1 mM Cu(II) solution to 0.013 s^{-1} when the ratio of [SDS] / [Cu(II)] is 4 .

Among the three co-surfactants which were added to the copper(II) surfactant solutions , $C_{12}E_8$, is most potent in increasing the autooxidation rate of 3,5-DTBC . For example , when the ratio [$C_{12}E_8$] / [Cu(II)] increases from zero to 4 , the rate constant increases from $1.7x10^{-3}$ s^{-1} to $2.4x10^{-2}$ s^{-1} for the 0.5 mM [$Cu(C_{16}tmed)(acac)Cl$] system and from $1.2x10^{-2}$ to $1.5x10^{-1}$ s^{-1} for the 0.5 mM [$Cu(C_{12}tmed)Br_2$] system . In both cases , the rate is increased by at least an order of magnitude .

The plausible factors that would affect the autooxidation rate are discussed as below :

(1) Mixed micelles can synergically lead to a much greater solubilization of 3,5-DTBC than is possible through a homogeneous micelle formed from a single surfactant alone [61] . In principle , this would have the effect of increasing the observed autooxidation rate as the increased solubilization would bring together the various reacting species . However increasing amount of co-surfactant would increasingly dilute the copper(II) active species within the mixed micelle and thus retard the rate. The greater solubilization effect should be present in all the systems studied and it certainly plays an important role in the initial

sharp increase in rate when CTAB is added to the $[Cu(C_{12}tmed)Br_2]$ solution (Figure 3-52). The leveling-off at higher CTAB concentration is a result of the dilution effect.

(2) In the Stern layer where the copper(II) head group is , the initial addition of SDS would reduce the positive charge density in the head group region with a concomitant lowering of the pH value [101] and resulting in a retardation in rate [102] . On further addition of SDS , the fraction of SDS in the mixed-micelle increases [22(d)] and finally in the SDS-rich medium , the net charge density would become negative , leading to a further retardation in rate . This localized pH effect would certainly play a part in Cu(II) / SDS systems , but the opposite trend observed in the two mixed-chelate compounds suggests that this effect is not very important .

In the case of CTAB as a co-surfactant , the change in pH in the head group region is expected to be small because the charge density which always remains positive is governed mainly by the degree of counterion binding , which varies monotonically between the values of the pure ionic micelles [33(a)] .

On the addition of $C_{12}E_8$ to the copper(II) micelle , a reduction in the positive charge density in the head group region is expected , leading to a slight decrease in pH and a slight retardation in rate . Again , this cannot be invoked to explain the observed rate change .

(3) For the copper(II) surfactant at concentration above the CMC , the following equilibria can occur in the aqueous solution [11(b)] when the co-surfactants are SDS and CTAB :

In SDS ,

$$[Cu_nL_n(acac)_nCl_p]^{(n-p)+} + 2H_2O \rightleftharpoons [Cu_nL_{n-1}(acac)_nCl_p(H_2O)_2]^{(n-p)+} + L \qquad (3\text{-}49)$$

$$[Cu_nL_n(acac)_nCl_p]^{(n-p)+} + DS^- \rightleftharpoons [Cu_nL_{n-1}(acac)_nCl_p(DS)]^{(n-p-1)+} + L \quad (3\text{-}50)$$

$$[Cu_nL_{n-1}(acac)_nCl_p(H_2O)_2]^{(n-p)+} + DS^- \rightleftharpoons [Cu_nL_{n-1}(acac)_nCl_p(DS)]^{(n-p-1)+} + 2H_2O \quad (3\text{-}51)$$

In CTAB ,

$$[Cu_nL_n(acac)_nCl_p]^{(n-p)+} + 2Br^- \rightleftharpoons [Cu_nL_{n-1}(acac)_nCl_pBr_2]^{(n-p-2)+} + L \quad (3\text{-}52)$$

$$[Cu_nL_{n-1}(acac)_nCl_p(H_2O)_2]^{(n-p)+} + 2Br^- \rightleftharpoons [Cu_nL_{n-1}(acac)_nCl_pBr_2]^{(n-p-2)+} + 2H_2O \quad (3\text{-}53)$$

where n is the aggregation number of the micelle , p is the number of chloride ion associated with the head group and L = C_n-tmed . The magnitude of the equilibrium constant , K_{eq} , for equation (3-49) is expected to be larger when C_n in L is shorter because the hydrophilicity of L increases with a decrease in the alkyl chain length . Thus , in the [Cu(C_{12}tmed)(acac)Cl] case , K_{eq} is larger than that of the C_{16}-tmed analogue , leading to a greater extent of the formation of $[Cu_nL_{n-1}(acac)_nCl_p(DS)]^{(n-p-1)+}$ and hindering the formation of the copper(II)-catecholate complex , an intermediate formed in the pathway of copper(II)-catalyzed autooxidation of catechols [11(c)] . This would lead to a retardation in rate . The same kind of equilibrium also occurs in [Cu(C_{12}tmed)Br_2] (in the presence of SDS) but the above equilibria do not occur to an appreciable extent in the C_{16} case . This explanation can also be applied to account for a 7-fold retardation in the autooxidation rate of non-micellar [Cu(CH_3-tmed)(β-diketonate)]NO_3 solution in the presence of SDS [11(c)] .

(4) It has been reported that the solubility of molecular oxygen in the micellar phase is more than that in the bulk aqueous phase [103]. For a single surfactant solution , the solubility of oxygen in the micelle follows the order

$$\text{BRIJ-35 } (C_{12}E_{23}) << \text{SDS} \equiv \text{CTAB}$$

As far as we are aware , other than a study in the BRIJ-35 - BRIJ-30 mixed micelle system [103] , information on the effect of a co-surfactant on the solubility of gas in the mixed micelle is lacking in chemical literature . However , the observed increase in rate in $C_{12}E_8$ as co-surfactant and the smallest solubility of oxygen in BRIJ-35 , a polyethoxylated lauryl alcohol residue , seem to suggest that the increased O_2 solubilization does not play an important role at least in the cases of Cu(II) / $C_{12}E_8$ systems .

(5) A change in the reduction potential of copper(II) surfactant in the mixed micelle can also affect the rate . Although it is well known that the reduction potential of copper(II) increases in a micellar environment [7] , the effect of a co-surfactant on the redox potential of micellar copper(II) has not been reported . However , the redox potential of surface active N-hexadecyl-N'-methyl viologen ($C_{16}C_1V^{2+}$; 0.1 mM) solubilized in 5 % Triton X-100 , 50 mM CTAC and 50 mM SDS micelles had been determined to be -0.48 , -0.54 and -0.67 V respectively [104] . As both the micellized copper(II) complex and $C_{16}C_1V^{2+}$ are positively charged as well as both $C_{12}E_8$ and Triton X-100 are similar type of neutral surfactants where both have the similar hydrophilic oxyethylene groups, it is plausible that it is thermodynamically more favorable for the micellized copper(II) to be reduced to copper(I) in $C_{12}E_8$. This could account for the dramatic rate increase in the [Cu(C_{12}tmed)Br_2] and [Cu($C_n$tmed)(acac)Cl] cases in $C_{12}E_8$ as compared to those in the cationic and anionic co-surfactants .

From the above discussion , one can therefore conclude that the greater concentration effect of mixed micelle, the hydrophilicity effect of L on the multiple-equilibrium and the change in the reduction potential of Cu(II) in mixed-micelle are the major factors accounting for the observed change in rate .

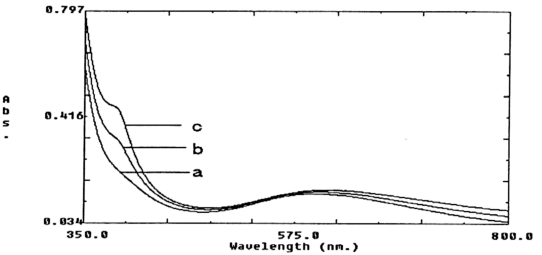

Figure 3-46 : UV spectra of 1 mM $Cu(C_{12}tmed)(acac)Cl$ and 4 mM SDS at 25°C and natural pH and with various concentrations of 3,5-DTBC (absorbance at 385 nm) :

a. no 3,5-DTBC (0.228) ; *b.* 4.9 x 10^{-5} M (0.335) ; *c.* 9.8 x 10^{-5} M (0.446)

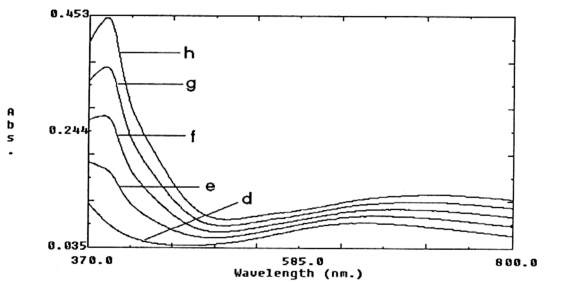

Figure 3-47 : UV spectra of 1 mM $Cu(C_{12}tmed)Br_2$ and 1 mM CTAB at 25°C and pH 6 and with various concentrations of 3,5-DTBC (absorbance at 385 nm) :

d. no 3,5-DTBC (0.086) ; *e.* 5 x 10^{-5} M (0.179) ; *f.* 1 x 10^{-4} M (0.272) ; *g.* 1.5 x 10^{-4} M (0.361) ; *h.* 2 x 10^{-4} M (0.449)

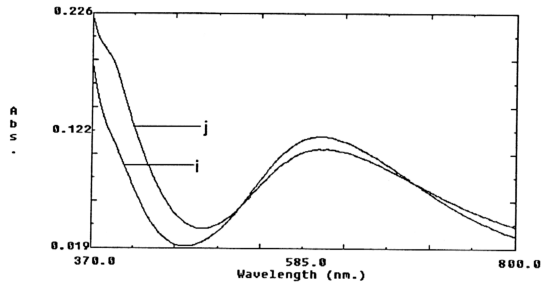

Figure 3-48 : UV spectra of 1 mM $Cu(C_{12}tmed)(acac)Cl$ and 4 mM $C_{12}E_8$ at 25°C and pH 5.7 and with various concentrations of 3,5-DTBC (absorbance at 385 nm) :

i. no 3,5-DTBC (0.127) ; *j.* 4.9 x 10^{-5} M (0.192)

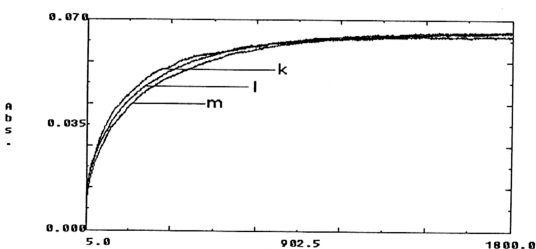

Figure 3-49 : Time course spectra for the autooxidation of 3,5-DTBC in the presence of 0.5 mM $Cu(C_{16}tmed)(acac)Cl$ with concentrations of CTAB :

k. 2 mM ; *l.* 1.15 mM ; *m.* 0.5 mM

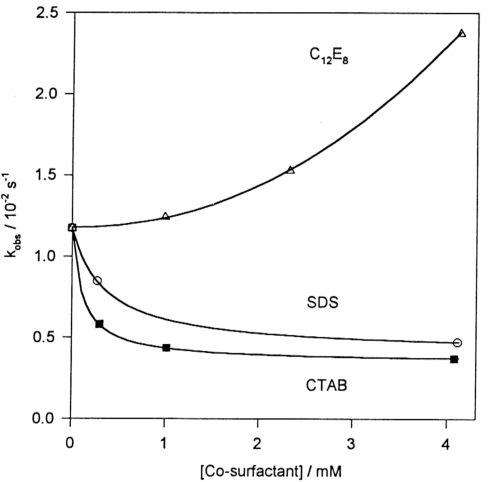

Figure 3-50 : Autooxidation rate of 3,5-DTBC in the presence of 1 mM $Cu(C_{12}tmed)(acac)Cl$ with various co-surfactants (25°C ; pH = 5.7) .

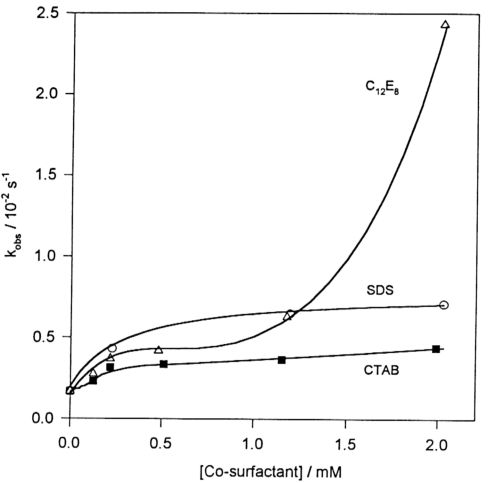

Figure 3-51 : Autooxidation rate of 3,5-DTBC in the presence of 0.5 mM $Cu(C_{16}tmed)(acac)Cl$ with various co-surfactants (25°C ; pH =5.7) .

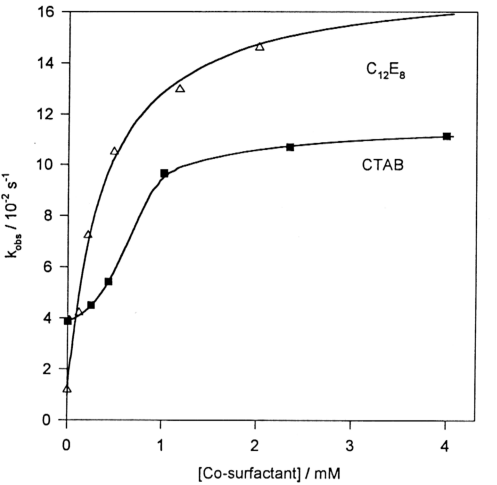

Figure 3-52 : Autooxidation rate of 3,5-DTBC in the presence of 0.5 mM $Cu(C_{12}tmed)Br_2$ with various co-surfactants (25°C ; pH = 5.7) .

(II) Hydrolysis of *p*-nitrophenyl diphenyl phosphate (PNPDPP)

The effects of SDS , CTAB and $C_{12}E_8$ on dephosphorylation or hydrolysis of PNPDPP in the presence of copper(II) metallomicelles had been studied . In the hydrolysis of PNPDPP , pH of the solution was not adjusted . The natural pH of the system varied slightly as the co-surfactant was added to the copper(II) surfactant solution . In SDS case , pH varied from 6.4 to 8.0 ; in CTAB and $C_{12}E_8$ cases , pH was almost constant at around 6.2-6.6 in all the solutions . Hydrolysis of PNPDPP will liberate p-nitrophenolate ion which was monitored at 400 nm . The UV spectra of formation of p-nitrophenol were shown in Figure 3-53 . Some more time course curves for the hydrolysis of PNPDPP are shown in appendix VI .

Table 3-32 : The values of k_{obs} for the hydrolysis of PNPDPP in the micellar solutions at 25°C

Compound	Concentration / 10^{-3} M	k_{obs} / 10^{-3} s^{-1}
SDS	1	1.1
CTAB	1	0.13
$C_{12}E_8$	1	0
$Cu(C_{12}tmed)(acac)Cl$	1	2.7
$Cu(C_{16}tmed)(acac)Cl$	1	4.5
$Cu(C_{12}tmed)Br_2$	1	10.6

As can be seen from Table 3-32 , the observed rate constant for the hydrolysis of PNPDPP at 25°C is higher in the presence of pure copper(II) metallomicelles when compared to non metallomicelles (i.e. SDS, CTAB, $C_{12}E_8$). The observed rate constants in the presence of copper(II) metallomicelles and co-surfactants are plotted against concentration of co-surfactant in Figures 3-54, 3-55 and 3-56 . In the

[$Cu(C_{16}tmed)(acac)Cl$] case , where the co-surfactant is SDS , the rate increases slightly to a maximum at ~ 0.25 mM concentration and followed by a gradual decrease . On the addition of CTAB and $C_{12}E_8$, however , the rate decreases . For the [$Cu(C_{12}tmed)Br_2$] and [$Cu(C_{12}tmed)(acac)Cl$] cases , except for the [$Cu(C_{12}tmed)Br_2$] / [SDS] system , in which the observed rate decreases sharply from 0.011 s^{-1} in pure 1 mM Cu(II) solution to 0.0013 s^{-1} on addition of 4 mM SDS , the observed rates exhibit a similar pattern , *viz.* they increase on adding small amount of the co-surfactant , reach a maximum at around 0.2-0.3 mM and decrease gradually on further addition of the co-surfactant .

Alkaline hydrolysis of PNPDPP in micelle had been studied by a lot of workers [45(a),45(b),58,62,76] . The observed rate of reaction depends on the amounts of substrate and reactive anion bound to the micelle and on the intrinsic second-order rate constants in the bulk aqueous phase and in the micellar pseudophase . The fraction of reactive anions bound to a cationic micelle depends on both the ion exchange selectivity of the micelle for the reactive anion , and on the fraction of counterion dissociated from the micelle .

Menger et. al. [7] proposed that the catalytically active nucleophile in the hydrolysis of PNPDPP came from OH of a hydroxo chelate ($Cu[L][OH]^+$) . They also suggested that the micellization can promote the electrophilicity of the cupric head group by polarizing the P = O group and thus enhanced the catalysis . pH-concentration profile for the copper micellar solution had been carried out by Lim et. al. [11(b)]. They suggested that the lowering of pH after the maximum is caused by deprotonation of copper(II)-bound water . This deprotonation has an effect of reducing the charge on the head group , and thus facilitating micellization . Bunton et. al. [2(g)] had tried to find the

source of catalysis of dephosphorylation of PNPDPP by metallomicelles . They synthesized a series of copper complexes of 2-(dimethylaminomethyl)-6-(alkylaminomethyl) pyridines , and compared the rate constants in their presence with Cu^{II} complexes of N,N,N'-trimethyl-N'-alkyl-ethylenediamine . The results indicate (i) the nucleophilicity of the L-Cu^{II}-OH species is similar in metallomicelles and monomeric complexes ; (ii) free OH^- is a slightly better nucleophile than Cu^{II}-bound OH^- in all complexes ; (iii) electrophilic assistance is only present in the monomeric complex and vanishes in metallomicelles .

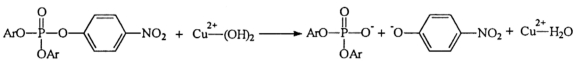

(3-54)

In our present systems , the following equilibria can also occur in the copper micellar solutions [11(b)] :

$$\left[CuL_n(acac)_n\right]^{n+} + pCl^- \rightleftharpoons \left[CuL_n(acac)_n Cl_p\right]^{(n-p)+} \tag{3-55}$$

$$\left[CuL_n(acac)_n\right]^{n+} + mH_2O \rightleftharpoons \left[CuL_n(acac)_n(H_2O)_m\right]^{n+} \tag{3-56}$$

$$\left[CuL_n(acac)_n(H_2O)_m\right]^{n+} \rightleftharpoons \left[CuL_n(acac)_n(OH)_m\right]^{(n-m)+} + H^+ \tag{3-57}$$

Deprotonation of copper(II)-bound water in Equation 3-57 will produce copper(II)-OH . Process that increases the effective concentration of the Cu(II)-OH species within the micelle would increase the rate of hydrolysis . The small increase in rate on addition of CTAB and $C_{12}E_8$ to [Cu(C_{12}tmed)Br_2] and [Cu(C_{12}tmed)(acac)Cl] is due to the increased micellization of the copper(II) surfactant with the resultant increase in the

solubilization of the substrate molecule . However , further addition of CTAB or $C_{12}E_8$ would dilute the effective concentration of Cu(II)-OH and thus reduce the rate . At 1 mM concentration , which is well above the CMC of [Cu(C_{16}tmed)(acac)Cl] , *viz.* , $4x10^{-5}$ M [11(d)] , the extent of micellization is sufficiently large so that any addition of CTAB or $C_{12}E_8$ would just dilute the Cu(II) effective concentration and reduce the rate .

The sharp decrease in rate when SDS is added to [Cu(C_{12}tmed)Br_2] solution is caused by the binding of sulfate oxygen to copper(II) center , thus preventing formation of Cu-OH species within the micelle .

In conclusion , this study shows that the addition of co-surfactant to copper(II) micelle only enhances slightly the hydrolysis rate of PNPDPP when a small amount of co-surfactant is added and that overall the co-surfactants have the rate-inhibition effect when added in increasing amount .

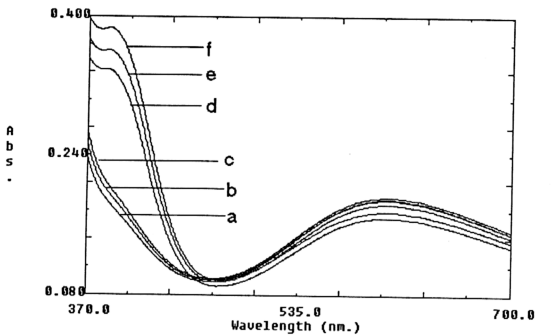

Figure 3-53 : UV spectra of 1 mM $Cu(C_{16}tmed)(acac)Cl$ at 25°C and natural pH with :

a. 0.26 mM SDS , no PNPDPP ; *d.* 0.26 mM SDS , with PNPDPP ;

b. 0.25 mM $C_{12}E_8$, no PNPDPP ; *e.* 0.25 mM $C_{12}E_8$ with PNPDPP ;

c. 0.26 mM CTAB , no PNPDPP ; *f.* 0.26 mM CTAB , with PNPDPP .

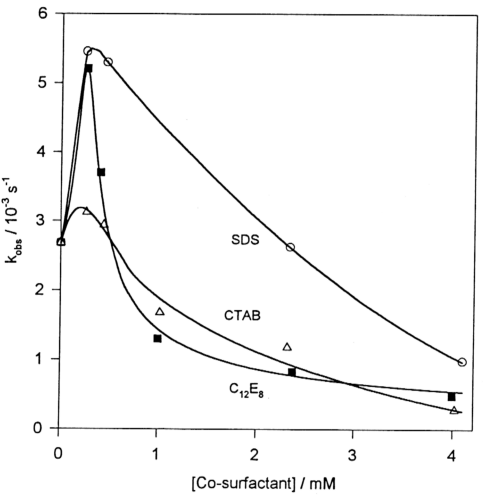

Figure 3-54 : Hydrolysis of PNPDPP in the presence of 1 mM $Cu(C_{12}tmed)(acac)Cl$ with various co-surfactants .

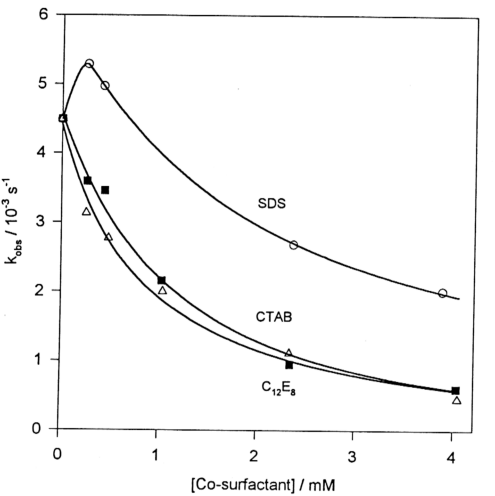

Figure 3-55 : Hydrolysis of PNPDPP in the presence of 1 mM $Cu(C_{16}tmed)(acac)Cl$ with various co-surfactants .

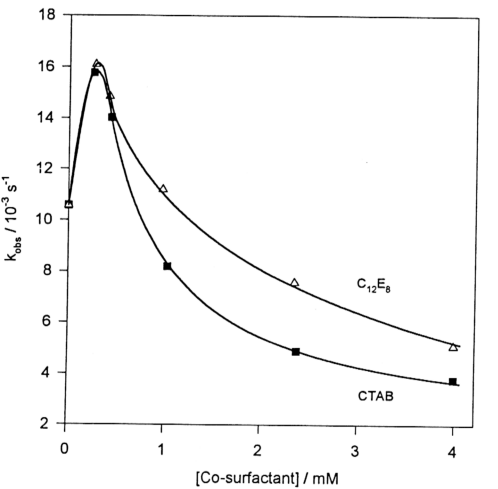

Figure 3-56 : Hydrolysis of PNPDPP in the presence of 1 mM $Cu(C_{12}tmed)Br_2$ with various co-surfactants .

(E) Conclusion

Various models have been applied to treat the surface tension data . In the Regular Solution approach , mutual interaction of the components in the mixed micelles was measured by micellar interaction parameter β^{M} . It was found that Cu / SDS mixtures show negative deviation from ideality , whereas Cu / CTAB and Cu / $C_{12}E_8$ systems almost mixed ideally . The strong interaction in the Cu / SDS mixtures is probably due to formation of electroneutral combination $R^{+}R^{-}$ ions . This ion pair is more surface active than $R^{+}Cl^{-}$ and $R^{-}Na^{+}$ and causes the decrease in CMC values .

In the mixed monolayer formation , the E-method $\beta^{\sigma,E}$ values vary with the surface tension values while the R-method $\beta^{\sigma,R}$ values are constant . We believe that the R-method is a better method of estimating molecular interaction in the mixed monolayer .

Among the three binary surfactant mixtures studied , only Cu / SDS system shows existence of synergism in surface tension reduction efficiency , mixed micelle formation and surface tension reduction effectiveness .

Besides the interaction parameters of the components in the mixed micelle , Regular Solution Model also provides information on the micellar and monolayer compositions . In the Gibbs-Duhem approaches (Motomura, Scamehorn, and Yu) only the micellar and monolayer compositions are determined . However , the composition values appear to be dependent on the choice of the method of graphical data analysis as is evident in the Cu / SDS system (Table 3-21(a)) .

UV-Vis and ESR studies show that the introduction of cosurfactant will displace some Cl^- anion in the mixed micelle . While pure micellar copper solution only gives rise to a broad signal at ~317 mT , additional sharp signal at ~326 mT was obtained for the mixed micelle solutions . We suggest that cosurfactant head group was inserted in between some of the copper head groups , with alternating block arrangement , i.e., one block with pure copper surfactant and another block with mixed surfactant .

In the kinetic studies , mixed Cu / $C_{12}E_8$ combination appears to be a good catalyst for the autooxidation of 3,5-di-*tert*-butylcatechol . However the rate of hydrolysis of *p*-nitrophenyl diphenyl phosphate is generally retarded by the presence of cosurfactant . In order to obtain better understanding on the kinetic behavior of the mixed micelles , it is proposed that kinetic investigations under the condition of varying total concentration (of both surfactants) but with constant mixing ratio are to be carried out in future work . It is envisaged that with a constant mixing ratio the structure of the head group remains constant or nearly constant as the total concentration changes . This type of rate study may throw some light on the effects of head group structure on the rate of reactions of the two substrate molecules that have been reported in this thesis .